FINAL TECHNICAL REPORT
October 1, 2007, through March 31, 2009

Project Title: UNDERSTANDING MULTI-INTERACTIONS OF SO_3, MERCURY, SELENIUM, AND ARSENIC IN ILLINOIS COAL FLUE GAS

ICCI Project Number:	07-1/6.1A-1
Principal Investigator:	Ye Zhuang, Energy & Environmental Research Center
Other Investigators:	Christopher L. Martin and John H. Pavlish, Energy & Environmental Research Center
Project Manager:	Dr. Francois Botha, ICCI

ABSTRACT

This project consisted of pilot-scale combustion testing with a representative Illinois Basin coal to explore the multi-interactions of SO_3, mercury, selenium, and arsenic. The parameters investigated for SO_3 and mercury interactions included different flue gas conditions, i.e., temperature, moisture content, and particulate alkali content, both with and without activated carbon injection for mercury control. Measurements were also made to track the transformation of selenium and arsenic partitioning as a function of flue gas temperature through the system. The results from the mercury–SO_3 testing support the concept that SO_3 vapor is the predominant factor that impedes efficient mercury removal with activated carbon in an Illinois coal flue gas, while H_2SO_4 aerosol has less impact on activated carbon injection performance. Injection of a suitably mobile and reactive additive such as sodium- or calcium-based sorbent was the most effective strategy tested to mitigate the effect of SO_3. Transformation measurements indicate a significant fraction of selenium was associated with the vapor phase at the electrostatic precipitator inlet temperature. Arsenic was primarily particulate-bound and should be captured effectively with existing particulate control technology.

EXECUTIVE SUMMARY

Copollutant removal of SO_2 and mercury across wet flue gas desulfurization (FGD) systems is considered to be a cost-effective way to control regulated emissions, especially since the SO_2 limits under the Clean Air Interstate Rule have resulted in a number of new wet FGD installations. However, field test data suggest that such plants will need additional or incremental Hg removal to meet the more restrictive mercury regulations that have been adopted in Illinois (approximately 90% removal), or which may be proposed nationally as Maximum Achievable Control Technology (MACT) standards. Activated carbon injection (ACI) has emerged as the most developed mercury control technology, and while it is cost-effective for many plants and coal types, ACI has not been successful with high-sulfur coals such as Illinois Basin bituminous coals. The hypothesis proposed in this work is that the SO_3 vapor generated from combustion of high-sulfur coal reacts with the carbon and hinders its ability to remove mercury. A thorough investigation of the multi-interactions among mercury, SO_3, and carbon under different flue gas conditions, i.e., temperature, moisture content, and particulate alkali content, was undertaken to explore the hypothesis.

The results from pilot-scale testing with a representative Illinois Basin coal support the concept that SO_3 vapor is the predominant factor that impedes efficient mercury removal with activated carbon in an Illinois coal flue gas, while H_2SO_4 aerosol has less impact on ACI performance. The poisonous effect of SO_3 on activated carbon appears to be from a direct competition between mercury and SO_3 for active sites on the carbon. The resulting effects on mercury capture with ACI can be explained by fundamental mass transfer effects. Although reducing flue gas temperature or increasing moisture level did counteract the deleterious effect of SO_3 vapor on ACI performance to some degree, injection of a separate additive to neutralize the SO_3 vapor was most promising. However, it is critical that the added species has sufficient reactivity and mobility to neutralize SO_3 in the short contact time available.

Native removal of mercury across the electrostatic precipitator (ESP) was observed to be less than 10%, and it was not significantly sensitive to any of the parametric test conditions. Unless a plant has a significant amount of unburned carbon in the flue gas, native mercury removal will not be a significant contribution to overall mercury control. Mercury exiting the ESP under baseline conditions was approximately 65% oxidized. Mercury oxidation was not found to be sensitive to the parametric test conditions, including ACI. More oxidation, and presumably more cobenefit removal in a wet FGD system, could be expected for systems employing a selective catalytic reduction unit, but this was not included in the pilot-scale configuration.

Following mercury, selenium and arsenic are likely to be the next two trace elements present in coal that will be regulated because of their adverse health and environmental effects and their relative volatility. Transformation measurements for these elements were made during pilot-scale testing with a representative Illinois Basin coal. The selenium transformation measurements indicate that while some of the selenium becomes particulate-bound there is still a significant fraction of selenium vapor remaining at an

ESP inlet temperature of 312°F. If selenium emissions become regulated, this fraction of selenium vapor may be very difficult to capture and would likely require the development of new technology. Transformation measurements for arsenic indicate that over 98% of the arsenic becomes particulate-bound by a temperature of 800°F and reaches 99.5% when the temperature reduces to 312°F. The arsenic was highly concentrated in submicrometer particles, but it should be effectively controlled with existing particulate control equipment.

OBJECTIVES

The overall project goal was to establish a fundamental understanding of the transformations and interactions of mercury, selenium, and arsenic in an Illinois coal combustion flue gas environment. The project specifically focused on the transformation of these elements as a function of the flue gas temperature profile from the boiler outlet to the particulate control inlet. Because of the immediate control challenge, mercury interactions were also evaluated under different parametric test conditions: temperature, sulfur trioxide (SO_3) concentration, moisture content, and particulate alkali content. By understanding the interactions and effects of flue gas constituents and their speciation, targeted strategies can be developed for plants burning Illinois coal to enhance any or all of the following:

- Native mercury capture by enhancing interactions with particulate matter, including unburned carbon in the flue gas.

- Mercury oxidation, both native and that resulting from interactions with injected sorbents, to ultimately result in increased capture in a downstream wet flue gas desulfurization (FGD) system.

- Mercury removal with cost-effective sorbent injection.

Specific objectives of the project were the following:

- Evaluate SO_3 partitioning between vapor and aerosol phases as a function of flue gas temperature, moisture content, and particulate alkali content.

- Quantify and facilitate mercury oxidation and/or native in-flight adsorption at varied SO_3 concentrations, with a target of approximately 70% mercury oxidation by changing flue gas temperature, moisture level, or alkali content in the Illinois coal flue gas.

- Quantify and facilitate mercury oxidation and/or in-flight adsorption on activated carbon at varied SO_3 concentrations with targets of approximately 90% mercury oxidation and approximately 80% in-flight mercury adsorption.

- Determine the partitioning (vapor versus particulate) of mercury, selenium, and arsenic in Illinois coal flue gas at temperatures from 800° to 300°F.

- Quantify size distributions (0.5–15 μm) of mercury, selenium, and arsenic in Illinois coal fly ashes collected at temperatures of 800°, 450°, and 300°F.

INTRODUCTION AND BACKGROUND

Copollutant removal of sulfur dioxide (SO_2) and mercury across wet FGD systems is considered to be a cost-effective way to control regulated emissions, especially since the SO_2 limits under the Clean Air Interstate Rule have resulted in a number of new wet FGD installations. This is particularly advantageous for users of Illinois Basin coal, since the coal's high sulfur content typically requires the use of a wet SO_2 scrubber. However, with the recent U.S. District of Columbia Circuit Court of Appeals decision to vacate the Clean Air Mercury Rule and individual states adopting more restrictive regulations, it is now doubtful that cobenefit removal alone can meet future mandated mercury removals.

The existing data from power plant sampling indicate that cobenefit removal alone achieved an average of 69% removal for plants with a cold-side electrostatic precipitator (ESP) followed by a wet FGD (1) (a typical configuration for plants using Illinois coal). The average removal increases to 85% for units that also incorporate selective catalytic reduction (SCR) (1). These data suggest that such plants will need additional or incremental Hg removal to meet the more restrictive mercury regulations that have been adopted in Illinois (approximately 90% removal) or which may be proposed nationally as maximum achievable control technology (MACT) standards.

As a result of research conducted over the last decade, several strategies have been developed and are now available to improve or increase mercury removal. Since it is possible that a plant with a wet FGD might only need an additional 5%–10% of mercury removal to meet tougher regulations, enhancing the removal efficiency of existing mechanisms within the plant may be a viable option. This route would include enhancing native mercury removal across the plant's particulate control device or increasing the amount of cobenefit removal in a wet FGD system. Another possibility is in-flight capture of mercury through the injection of a suitable sorbent into the flue gas. Activated carbon has been the most widely used sorbent because of its acceptable combination of mercury capture efficiency and consumable cost.

While mercury control using activated carbon injection (ACI) can be a cost-effective removal option, it may not be an available tool for users of Illinois coal because of its inadequate performance with high-sulfur bituminous coals. Several mercury field tests using ACI have shown poor mercury removal at sites with substantial concentrations of either native SO_3 produced during the combustion of high-sulfur bituminous coals or SO_3 injected for ash conditioning (2).

One possible reason ascribed to this poor sorbent performance with the high-sulfur bituminous coal flue gas is the interaction with SO_2, where speculated interactions between SO_2 and Cl_2 obstruct chlorine-promoted mercury oxidation and the gas-to-particle conversion of mercury (3). Moreover, SO_2 is capable of impeding mercury adsorption onto particulate matter including AC and other flue gas solids by competing for adsorption sites on the particulate matter (4). However, SO_2 alone does not account for poor ACI results. Bituminous coal containing medium-to-high sulfur levels, such as Illinois Basin coal, will produce a significant amount of SO_3 in flue gas during

combustion. Also, installed de-NO_x SCR units catalytically oxidize some SO_2 into additional SO_3 in coal flue gas. It is believed that SO_3, although at a much lower concentration than SO_2 in flue gas, plays a critical role during in-flight capture of mercury with ACI since SO_3 may have a faster binding rate than SO_2 on the activated sites of AC. SO_3 in flue gas can exist either as a vapor or a condensed sulfuric acid mist (H_2SO_4 aerosol), depending on the temperature and moisture content of the flue gas. SO_3 vapor can also condense on existing fly ash particles where the condensation rate is determined by particle size, envelop surface area, and chemical characteristics of the in-flight particles. As a result of the faster diffusion rate toward in-flight particles, including injected AC, the adverse effect of SO_3 vapor on mercury in-flight adsorption is expected to be more severe than for sulfuric acid aerosols.

The adverse effect of SO_3 on mercury transformation has made mercury emission control for plants burning Illinois coal very challenging. To determine plant operating conditions that will facilitate mercury control, SO_3 partitioning between vapor and aerosol phases as well as its impact on mercury transformations needs to be understood as a function of flue gas temperature and moisture content. A comprehensive understanding regarding the interactions of SO_3, mercury, and in-flight alkali and alkaline-earth-based particles will facilitate the development of effective mercury control strategies for utility plants burning Illinois coal.

Following mercury, selenium and arsenic are likely to be the next two trace elements present in coal that are of interest because of their adverse health and environmental effects and their relative volatility. These toxic elements can be found in a coal's organic matrix such as organometallic salts or as mineral inclusions in coal. Like mercury, selenium and arsenic compounds are vaporized during coal combustion and leave the combustion zone as a vapor. The speciation of arsenic and selenium in coal flue gas depends on both the flue gas temperature and other flue gas constituents. Thermal equilibrium calculations (5) indicate that SeO(g) and SeO_2(g) are the dominant species in coal flue gas over 350°F, while for arsenic, AsO(g) is the only dominant species over 1250°F, and solid arsenates such as $AlAsO_4$ and Mg_2AsO_8 are formed when flue gas temperature is below 1250°F. Available data with other coals indicate that part of the selenium in flue gas may remain as a gas and exit the stack, while most of the arsenic is generally found in the solid phase and is collected in particulate control equipment (6).

EXPERIMENTAL PROCEDURES

Description of Test Facility and Methods

Pilot-Scale Combustor. Pilot-scale testing was conducted with the Energy & Environmental Research Center's (EERC's) particulate test combustor (PTC), a 550,000-Btu/hr pulverized coal-fired unit designed to generate flue gas and fly ash representative of that produced in a full-scale utility boiler. A diagram of the PTC is provided in Figure 1. The combustor is oriented vertically to minimize wall deposits. A refractory lining helps to ensure adequate flame temperature for complete combustion and prevents rapid quenching of the coalescing or condensing fly ash. Based on the superficial gas velocity, the mean residence time of a particle in the combustor is approximately 3 seconds. The coal nozzle of the PTC fires axially upward from the bottom of the combustor, and secondary air is introduced concentrically to the primary air with turbulent mixing. Coal is metered into the primary airstream via a gravimetric screw feeder and eductor. An electric air preheater is used for precise control of the combustion air temperature. The temperature of the flue gas is controlled downstream of the combustor through the use of heat exchangers and electric heat tracing. The temperature set points are designed to mimic the temperature profile of flue gas exiting a full-scale boiler, passing through an air preheater, and subsequently cooling before the particulate control equipment. In the PTC, the coal feed rate is adjusted to maintain a target volume flow of flue gas through the system. This maintains flue gas residence times and velocities in the system for consistent and representative testing.

As indicated in Figure 1, the PTC has a variety of particulate control options, but for this work, the configuration used was a cold-side ESP only with sorbent and additive injection upstream of the ESP. In this configuration, flue gas exiting the combustor passes through a series of heat exchangers and is then routed through a single-wire, tubular ESP. The ESP is designed to provide a specific collection area of 125 ft^2/kacfm at 300°F. Since the flue gas flow rate for the PTC is 130 scfm, the gas velocity through the ESP is 5 ft/min at 300°F. Plate spacing for the unit is 11 in. Sight ports are located at the top of the ESP to allow for online inspection of electrode alignment, sparking, rapping, and dust buildup on the plate. The ESP was designed to facilitate thorough cleaning between tests so that all tests can begin on the same basis.

The PTC instrumentation permits system temperature, pressure, flow rate, flue gas constituent concentration, and particulate control device (ESP and/or fabric filter [FF]) operating data to be monitored continuously and recorded on a data logger.

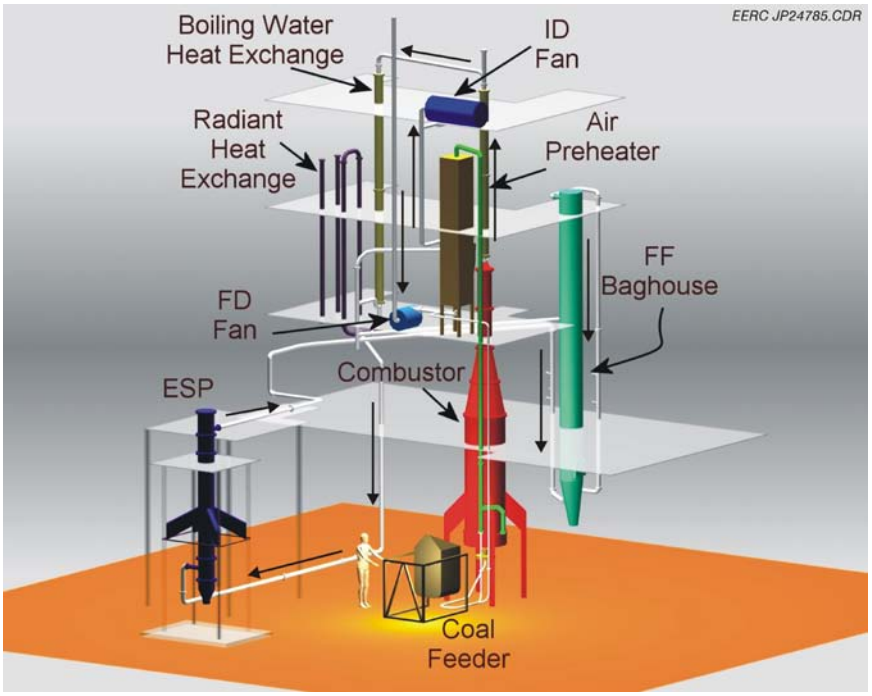

Figure 1. The EERC's PTC configured with an ESP–FF arrangement (FF not used for this testing).

Flue Gas Composition Analyses. Two emission monitors were used to obtain O_2, CO, CO_2, SO_2, and NO_x concentration data while the test coal was fired. O_2, CO, CO_2, and NO_x were determined using identical Rosemount Analytical NGA-2000 MLT3 multicomponent continuous gas analyzers, while the SO_2 was determined using analyzers manufactured by Ametek. Each of these analyzers were regularly calibrated and maintained to provide accurate flue gas concentration measurements. The sampling locations for these monitors were at the combustor outlet and downstream of the ESP outlet.

Mercury Speciation Measurement. Flue gas mercury concentrations were measured with two Tekran (Model 2537A) continuous mercury monitors (CMMs), with one instrument sampling at the ESP inlet and the other at the ESP outlet. Ontario Hydro (OH) measurements were taken at the ESP inlet and outlet at appropriate intervals during testing to provide verification of CMM data and detailed Hg speciation data. Total Hg values were also measured with U.S. Environmental Protection Agency (EPA) Method 29 (M29) samples, which were used to collect trace element partitioning data.

SO_3 Measurement. Flue gas SO_3 measurements were collected using a modified controlled condensation technique designed to measure the partitioning of sulfuric acid (H_2SO_4) aerosols and SO_3 vapor (7). As shown in the schematic of the SO_3 sampling arrangement (Figure 2), flue gas was sampled through a heated quartz filter followed by a temperature-controlled condenser that is loosely packed with glass wool. The first-stage filter, maintained at a temperature above the acid dew point, was to separate H_2SO_4 aerosol and any other particle-bound SO_3, assuming condensed SO_3/H_2SO_4 was enriched

in fine-sized particulates. While the second-stage condenser, controlled at 140°F, selectively condensed SO_3/H_2SO_4 vapor without capturing SO_2 or water in flue gas. The impinger train used was similar to those used in EPA Method 6; the first two are filled with 20 mL of 3% hydrogen peroxide to capture SO_2. These impingers are followed by one empty and one silica gel-filled impinger. After exiting the impingers, the dried gas sample passes through a dry gas test meter for accurate volume measurement. Sampling times were kept to 30 minutes in order to minimize any possible filter cake effects on the sampling results. Sulfate analysis of the quartz filter and condensate samples was used to determine the original amount of SO_3/H_2SO_4 in the flue gas. Sulfate concentration of the first-stage filter was determined to have been condensed H_2SO_4 aerosol, while the concentration in the second-stage condenser was declared the original SO_3 vapor concentration.

HCl Measurement. HCl concentration in flue gas was measured with one HCl analyzer (Thermo Environmental Instrument Model 15C) sampling at the ESP outlet. Hourly averages were reported to indicate temporal variation of HCl in flue gas during the testing period.

Partitioning of Trace Elements. EPA M29 measurements were taken to characterize the trace element partitioning between the particulate matter and vapor phase at three temperature profile points throughout the system. The trace elements of interest for this work were mercury, selenium and arsenic. Distributions of the three elements within fly ash were also determined. Particle-size distribution measurements were made using multicyclones followed by trace element analysis. The use of cyclones allowed larger samples of the particulates to be collected and allowed for trace element analysis of the collected particulate fractions.

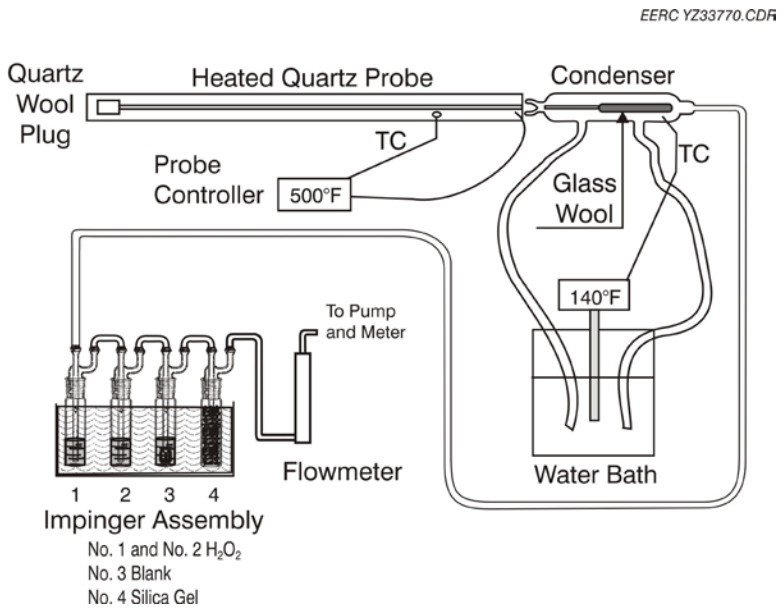

Figure 2. Schematic of the SO_3-sampling arrangement.

Test Plan

The pilot-scale testing took place over two 1-week periods for a total of nine testing days. The first period was July 14–18, 2008, and the second period was July 28–31, 2008. The matrix of tests conducted during the 2-week period is presented in Table 1 and divides the testing into four test series.

Test Series I, II, and III were designed to parametrically evaluate the effects of flue gas temperature, flue gas moisture level, and alkali addition, respectively, on SO_3–mercury interactions. The test conditions outlined in Table 1, e.g., moisture and alkali ratio, were nominal target values; postprocessing of the data determined the values actually obtained. Test Series IV was separate from the SO_3–mercury interaction work and was designed to measure the transformation mechanisms of mercury, selenium, and arsenic in Illinois coal flue gas.

Table 1. Completed Pilot-Scale Test Matrix

	Operating Parameters				Sampling Activities	
Test Series	ESP Temp., °F	Flue Gas Moisture, %	ACI, lb/Macf	Nominal Alkali Injection, Alkali/SO_3	OH	SO_3
I-1	250° 300° 350°	8.5	None	None	1 at ESP inlet 3 at ESP outlet	3 sets at ESP inlet/outlet
I-2	250° 300° 350°	8.5	5	None	1 at ESP inlet 3 at ESP outlet	3 sets at ESP inlet/outlet
II-1	300°	8.5 19–22[a]	None	None	1 at ESP inlet 3 at ESP outlet	2 sets at ESP inlet/outlet
II-2	300°	8.5 19–22[a]	5	None	1 at ESP inlet 3 at ESP outlet	2 sets at ESP inlet/outlet
III-1	300°	8.5	None	1:1 5:1 10:1	1 at ESP inlet 3 at ESP outlet	3 sets at ESP inlet/outlet
III-2	300°	8.5	5	1:1 5:1 10:1	1 at ESP inlet 3 at ESP outlet	3 sets at ESP inlet/outlet
IV	EPA M29 and multicyclone samples were collected in baseline flue gas at locations having 800°, 450°, and 300°F temperatures.					

[a] The original intent was to test two distinct moisture values above baseline; however, this is the actual achieved test range. Details are provided in the text.

Experimental Procedure

The coal combustor will be pre-heated using natural gas before the pilot-scale test. An approximately 65 lb/hr Illinois coal was then be fed into the coal combustor while the natural gas was shut off. A fine tuning-up on coal feed rate, primary and secondary air will be made to achieve complete coal combustion by continuously monitoring flue gas composition at the combustor outlet. Having established a stable and consistent combustion flue gas was then introduced into the pilot scale ESP with power on. Flue gas temperature across the entire pilot-scale system were continuously measured by thermocouples installed at different locations, e.g. combustor outlet, heat exchanger, ESP inlet, ESP middle section, and ESP outlet.

For each testing condition, the system will be operated for at least two-four hours to allow the system reaching stable condition before any planned flue gas samples including Mercury OH, SO_3, and Method 29 and Multicyclone were collected. Mercury CMM and HCl analyzer monitored flue gas continuously during the entire testing period. At the end of each test, the system was offline for a short time period to retrieve fly ash from the ESP.

RESULTS AND DISCUSSION

Coal Analyses. The coal used for these tests was an Illinois coal obtained from Knight Hawk Coal Company headquartered in Percy, Illinois. The coal was selected with the input of the Illinois Clean Coal Institute (ICCI) to ensure that it was acceptable in terms of being a representative Illinois Basin coal. During the 2-week pilot-scale run, daily composite coal samples were collected, and four of those samples were analyzed for proximate and ultimate analyses, heating value, chlorine, and the trace elements of interest: mercury, selenium, and arsenic. The results are summarized in Table 2.

As suggested by the results of Table 2, the coal properties were fairly consistent and are typical of an Illinois Basin coal, with an average 3.6% sulfur content and a heating value of approximately 11,000 Btu/lb on an as-fired basis. Chlorine content was lower than expected. However, there was more chlorine present than in low-chlorine coals, i.e., most subbituminous coals and lignites, which have typical chlorine concentrations less than 50 ppm.

Table 2. Summary of Coal Analyses for the Illinois Pilot-Scale Testing

	Sample 1 Week 1	Sample 2 Week 1	Sample 3 Week 2	Sample 4 Week 2	Average
Proximate Analysis					
Moisture, %	6.5	6.6	7.3	6.4	6.7
Volatile Matter, %	33.77	34.08	32.8	33.42	33.52
Fixed Carbon, %	48.22	48.47	46.33	47.02	47.51
Ash, %	11.51	10.85	13.57	13.16	12.27
Ultimate Analysis					
Hydrogen, %	5.32	5.33	5.22	5.4	5.32
Carbon, %	63.76	64.28	61.14	62.22	62.85
Nitrogen, %	1.37	1.35	1.32	1.32	1.34
Sulfur, %	3.63	3.55	3.64	3.7	3.63
Oxygen, %	14.41	14.64	15.11	14.2	14.59
Ash, %	11.51	10.85	13.57	13.16	12.27
Heat Value (Btu/lb)	11,162	11,268	10,612	10,810	10,963
Chlorine (µg/g), dry	140	143	134	131	137
Trace Elements of Interest					
Mercury (µg/g), dry	0.0904	0.0858	0.0871	0.0864	0.0874
Selenium (µg/g), dry	2.85	2.67	3.12	3.13	2.94
Arsenic (µg/g), dry	2.94	2.77	3.22	3.14	3.02

Note: all values on an as-fired basis unless otherwise noted.

The same daily composite coal samples were also ashed and analyzed for major inorganic elements using the wavelength-dispersive x-ray fluorescence spectrometer (WDXRF) technique. The analysis data are summarized in Table 3. The data indicate that the tested coal has a significant amount of Fe_2O_3 but low contents of alkali and alkaline-earth elements.

Flue Gas Composition. Table 4 presents the typical flue gas composition as measured at the combustor outlet. The PTC is operated with an excess oxygen concentration of 4%–5% to ensure that there is minimal unburned carbon leaving the combustor which could dramatically (and unpredictably) affect flue gas mercury concentrations. The measured SO_2 concentration is in fair agreement with a theoretical coal-derived value. An equilibrium calculation assuming all of the sulfur in the coal (3.63% average value) was converted to SO_2 results in an estimated dry flue gas concentration of 3900 ppmv, while the typical SO_2 concentration was measured as 3470 ppmv. The measured 9.11 ppmv HCl also agrees fairly well with the theoretical coal-derived value of 11.3 ppmv; however, it is lower than the typical HCl concentration in a bituminous coal flue gas.

Validation of CMM Data. The CMM was the primary source of mercury data, but periodic OH samples were also collected to verify the CMM values. In general, agreement between the CMM and OH samples was very good in terms of total gas-phase mercury concentration and the percentage of oxidized mercury.

Table 3. Major Inorganic Elements for Illinois Pilot-Scale Testing

Oxides, wt %	Sample 1 Week 1	Sample 2 Week 1	Sample 3 Week 2	Sample 4 Week 2	Average
SiO_2	53.0	53.2	53.1	53.0	53.08
Al_2O_3	23.8	23.7	23.2	23.4	23.52
Fe_2O_3	16.98	17.1	16.90	16.93	16.98
TiO_2	0.86	0.85	0.85	0.86	0.86
P_2O_5	0.23	0.22	0.26	0.26	0.24
CaO	2.0	1.8	2.4	2.4	2.15
MgO	1.05	1.06	1.07	1.07	1.06
Na_2O	0.20	0.20	0.21	0.20	0.20
K_2O	1.91	1.90	1.96	1.97	1.94

Table 4. Typical Flue Gas Composition at the Combustor Outlet

O_2, dry, vol%[a]	4.6
CO_2, dry, vol%	14.2
SO_2, dry, ppmv	3470
NO_x, dry, ppmv	768
CO, dry, ppmv	4.6
HCl, dry, ppmv[b]	9.11
Moisture, %[c]	8.5

[a] Regulated by pilot plant operators to ensure minimal unburned carbon.
[b] Measured at ESP outlet.
[c] Determined from baseline, ESP inlet OH samples.

Figure 3 is a graphical comparison of the baseline CMM and OH data along with the calculated flue gas Hg concentration based on the average coal mercury concentration presented in Table 2. Baseline conditions were considered to be the as-fired flue gas composition, i.e., no moisture or other additive addition, at a temperature of 300°F across the ESP. The ESP inlet data of Figure 3 are averages corresponding to the three OH measurements made at this location. Only one baseline OH measurement was collected at the ESP outlet (all other ESP outlet data were under test conditions); therefore, the outlet values in Figure 3 correspond to a single OH measurement.

Figure 4 is a graphical comparison of the remaining ESP outlet OH data and the corresponding CMM averages collected under various test conditions. The overall average relative percentage difference (RPD) for the total gas-phase data in Figure 4 was 4%, and all individual RPDs were within 15%. Mercury speciation data were also in good agreement, RPDs for OH and CMM-derived speciation values were typically less than 5%.

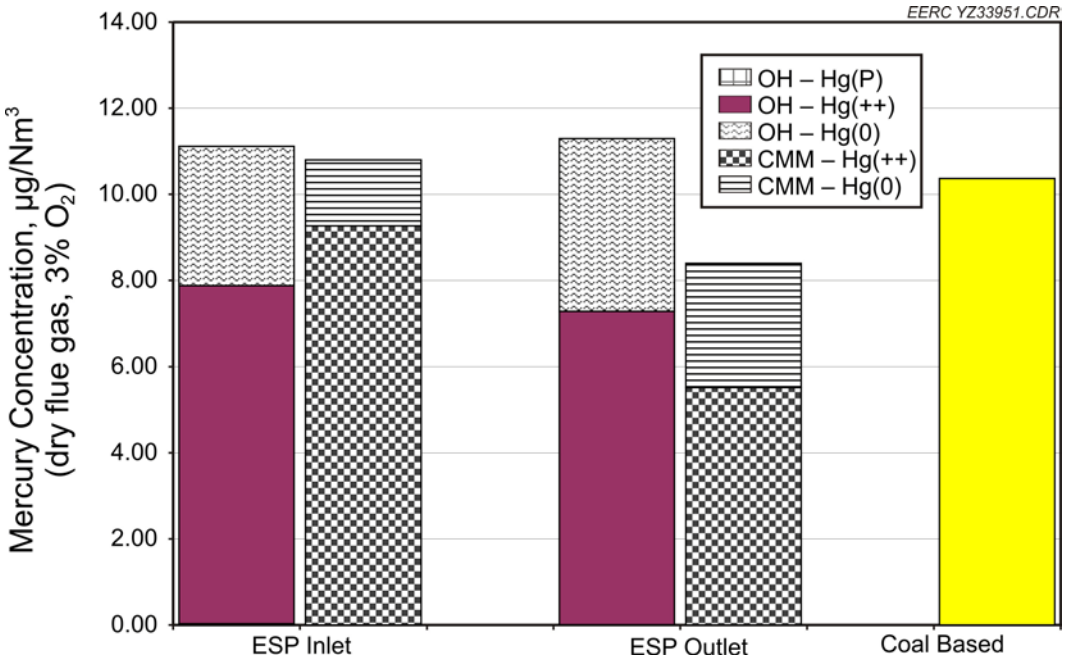

Figure 3. Comparison of CMM and OH flue gas mercury measurements during baseline conditions (8.5% moisture of flue gas and 300°F across the ESP).

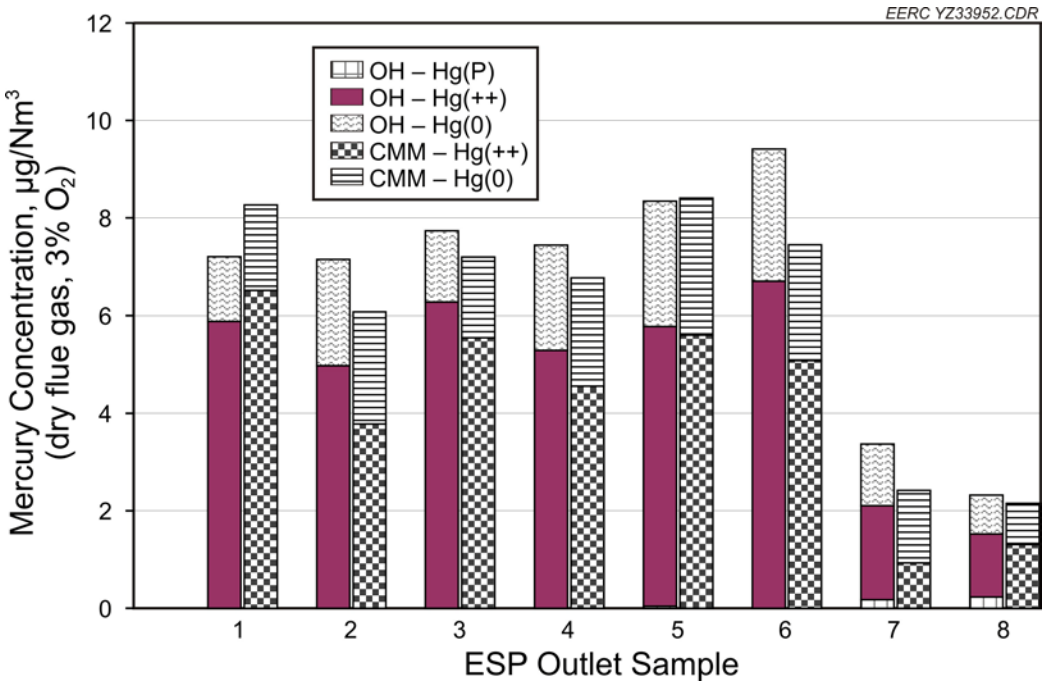

Figure 4. Comparison of ESP outlet OH measurements and the corresponding average CMM data.

Baseline Conditions. The baseline conditions for this test were considered to be the as-fired flue gas composition, i.e., no moisture or other additive addition, at a temperature of 300°F across the ESP. Mercury concentration, ACI performance, and SO_3 concentration were evaluated for this baseline condition.

Mercury Speciation Measurement. Measurements of baseline mercury concentration indicate that there was little native Hg removal across the ESP. The CMM data of Figure 3 show approximately a 10% removal, and the OH data indicate zero mercury removal during baseline. The coal-based mercury flue gas concentration is in good agreement with the ESP inlet measurements, qualitatively confirming that virtually all of the mercury present in the coal was vaporized and left the combustor with the flue gas.

Detailed baseline mercury speciation data are provided in Table 5, which is a summary of the OH-measured constituents of the total mercury. As shown, a majority of the mercury was detected in an oxidized form and is a consistent result for this Illinois bituminous coal with medium chlorine and high iron content.

The speciation data of Table 5 provide an example of the need for supplementary mercury control technology for plants burning Illinois coal. A plant with a wet scrubber installed could expect a maximum native mercury capture of approximately 70%–80%, assuming the mercury speciation of Table 5; however, this level of mercury removal will not meet Illinois' state mercury regulation of 90% removal.

Mercury Capture by Activated Carbon Injection. The baseline condition of 300°F also corresponded to one of the flue gas temperatures of Test Series I-2, so the detailed results of ACI testing are presented in the context of those results. In summary, two commercial ACs, an untreated AC, DARCO Hg, and a treated carbon, DARCO Hg-LH, were examined under the baseline condition, and both showed poor mercury capture performance. Maximum observed mercury removals were 35% at high injection rates greater than 15 lb/Macf.

Partitioning of SO_3 in Baseline Flue Gas. One set of SO_3 measurements were taken at the ESP inlet and outlet at the baseline condition and during ACI. These results are summarized in Table 6. The SO_3 ESP inlet data in the table are the average values for both sets of SO_3 measurements. As indicated by the results, the condensed SO_3 (H_2SO_4 aerosol) was effectively removed by the ESP, along with a significant portion of the SO_3 vapor. The removal of SO_3 vapor may partially be due to an altered equilibrium of vapor and aerosol phases across the ESP since it was operated within a ±10°F tolerance during the testing. The outlet result with ACI indicates that an additional 5.5 ppmv of vapor-phase SO_3 was removed by the carbon. The aerosol H_2SO_4 levels remained low with ACI.

Table 5. Baseline OH Mercury Speciation Data[a] for the Illinois Coal Flue Gas

	Particulate Hg, μg/dNm^3	Oxidized Hg, μg/dNm^3	Elemental Hg, μg/dNm^3	Total Hg, μg/dNm^3	Percent Oxidized
ESP Inlet [b]	0.03	7.85	3.23	11.08	71
ESP Outlet [c]	0.003	7.28	4.02	11.30	64

[a] All values normalized to 3% O_2.
[b] Average of three inlet measurements.
[c] Single outlet baseline value.

Table 6. Summary of Baseline SO_3 Partitioning Measurements Across the ESP (300°F)

	Vapor SO_3, ppmv[a]	Condensed SO_3 (H_2SO_4 equivalent), ppmv[a]	Total SO_3, ppmv[a]
ESP Inlet	28	93	121
ESP Outlet—Baseline	15.5	1.5	17
ESP Outlet—With ACI[b]	10	1	11

[a] All results are on a dry basis and normalized to 3% O_2.
[b] 5 lb/Macf DARCO Hg-LH.

Flue Gas Temperature Effect. Flue gas temperature was evaluated as a parameter to investigate mercury concentration and removal and SO_3 partitioning. ESP temperatures above and below the baseline condition of 300°F were investigated, i.e., 350° and 250°F, respectively.

Mercury Speciation Across ESP at Different Temperatures. The mercury concentration data for the ESP temperatures evaluated are presented in Table 7. The effect of flue gas temperature alone had little impact on the total concentration of mercury in the gas phase, considering the uncertainty of the CMM readings. Also, no significant native removal was observed for any of the temperatures.

Activated Carbon Injection at Different Temperatures. Mercury control using AC was tested for all three temperatures. Figure 5 is a summary of this testing, which is a plot of coal-to-ESP outlet Hg removal versus ACI rate. Two carbons were tested at the baseline temperature of 300°F, the untreated DARCO Hg and the treated DARCO Hg-LH, two commercially available carbons provided by Norit, Inc. It would appear from Figure 5 that the untreated AC performed slightly better than the treated option, but given the small difference and some day-to-day variation, these results are considered essentially the same. Maximum removals with either AC were less than 35%, even with very high injection rates. Only the DARCO Hg-LH was tested at the other temperatures. At the high-temperature condition, 350°F, mercury removal was essentially the same as at 300°F; however, a dramatic improvement in mercury removal was observed when the temperature was lowered to 250°F. At this temperature and an injection rate of 5 lb/Macf, mercury removal was observed to be greater than 40% and, at very high rates, the removal appeared to plateau at a value greater than 60%. Mercury speciation data at the ESP outlet during the ACI testing were included in Table 7.

Table 7. Averaged CMM Concentration Data Across the ESP at Different Temperatures

ESP Temp., °F	ESP Inlet Total Hg, µg/dNm^3	ESP Inlet Elemental Hg, µg/dNm^3	ESP Inlet % Oxidized	ESP Outlet Without ACI Total Hg, µg/dNm^3	ESP Outlet Without ACI Elemental Hg, µg/dNm^3	ESP Outlet Without ACI % Oxidized	ESP Outlet with ACI[a] Total Hg, µg/dNm^3	ESP Outlet with ACI[a] Elemental Hg, µg/dNm^3	ESP Outlet with ACI[a] % Oxidized
250	9.4	2.0	79	10	3.5	65	6.1	2.3	62
300	9.4	2.1	78	9.1	3.2	65	8.6	3.5	60
350	8.9	1.3	85	9.1	2.0	78	8.3	1.7	79

[a] DARCO Hg-LH at a rate of 5 lb/Macf.

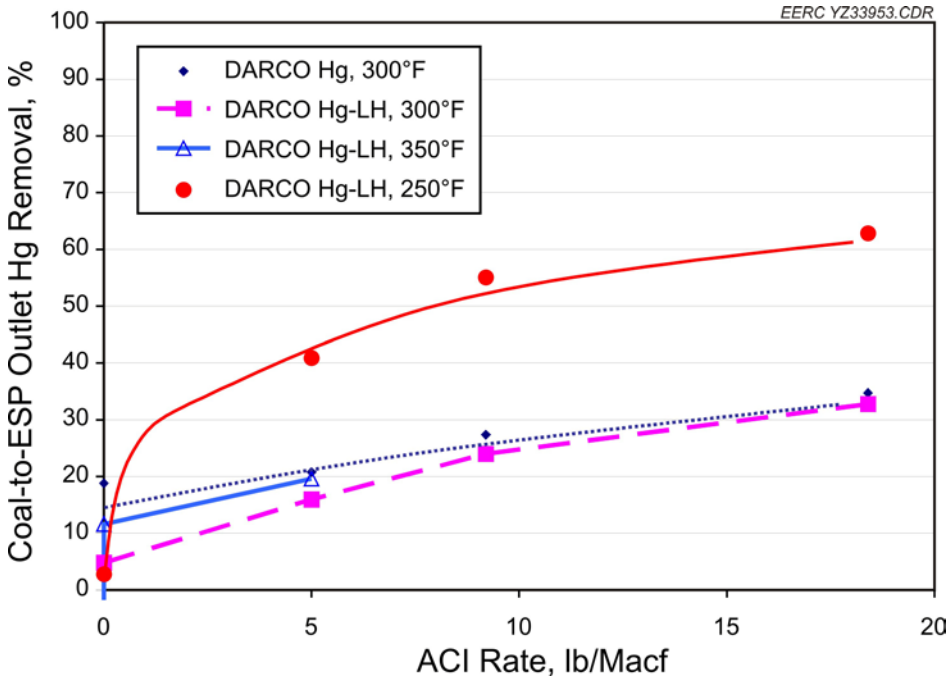

Figure 5. Summary of ACI testing with various ESP temperatures.

SO_3 Partitioning. Flue gas SO_3 measurements were taken at each ESP temperature evaluated; a paired set of measurements was taken across the ESP with and without ACI. The results of these measurements are presented in Figure 6. Assuming that a relatively constant fraction of the total sulfur in the coal is oxidized to form SO_3 in the combustor, it would be expected that the total amount of SO_3 and H_2SO_4 in the flue gas should be approximately constant (on a molar basis). The data of Figure 6 are roughly consistent with that hypothesis, considering the ESP inlet measurements, i.e., all of the inlet totals are within ±20% of the average, 131 ppmv. However, the distribution between vapor and aerosol phases is not constant and shows a trend with temperature; specifically, the amount of SO_3 in the vapor phase increases with temperature. The ESP outlet values are universally lower and suggest that nearly all of the aerosol H_2SO_4 is removed along with a smaller portion of the vapor SO_3. The addition of ACI removes a small amount of additional vapor-phase SO_3. The amount of exiting SO_3 vapor also appears linked to temperature, but this may not be a direct relationship since the amount of SO_3 vapor entering the ESP also increases with temperature.

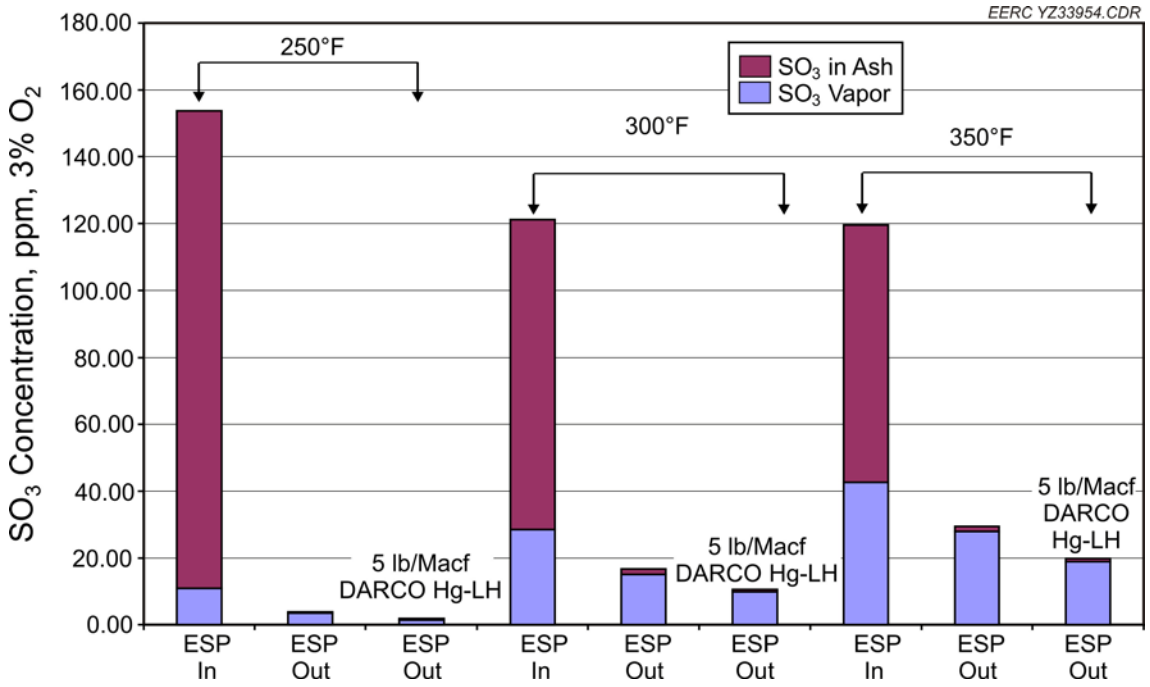

Figure 6. SO_3 sampling results for the ESP temperature test series.

The measured SO_3 vapor concentrations during the flue gas temperature test series have been plotted in Figure 7, along with the calculated SO_3 vapor equilibrium. The calculations of SO_3 vapor and H_2SO_4 equilibrium are based on the correlation proposed by Banchero and Verhoff (8). Overall, the data agree with the predicted trend in SO_3 vapor concentration; they show that lowering temperature was effective at altering the SO_3 partitioning by an order of magnitude. In comparison to the calculated values, the measured SO_3 vapor concentrations at 350°F were far below the equilibrium point, indicating that the flue gas was capable of containing extra SO_3 vapor. At the other extreme, the data at 250°F were above the saturation curve, suggesting that too much SO_3 vapor was present and condensation to H_2SO_4 should occur. Compared to the acceptable agreement observed at 300°F, it seems that equilibrium was not achieved for the other two temperatures; perhaps reaching equilibrium was prevented kinetically or because of irreversible SO_3/H_2SO_4 adsorption on fly ash. Additionally, both the experimental uncertainty (e.g., the temperature control tolerance across the ESP) and the uncertainty associated with the empirical formulation for calculating SO_3 equilibrium data could be contributing factors.

Flue Gas Moisture Addition. The amount of moisture in the flue gas was increased through steam injection to investigate the effects of humidity on mercury concentration and capture, SO_3 partitioning, and corresponding ACI performance. The unaltered flue gas moisture content was determined to be 8.5%, based on an average of the moisture values obtained from OH sampling. Moisture was added to the flue gas by injecting steam from the house supply into the combustor outlet. Steam flow was regulated by an existing steam supply subsystem at the EERC. This system controlled steam flow with a pneumatically actuated throttling valve and received feedback from a calibrated orifice

meter. This system regulated flow well; however, it was oversized for this purpose, and the achievable resolution between steam flow settings was poor. As a result, two distinct moisture levels (above baseline) were not obtained; instead, the results are better presented as one high-moisture condition, with a flue gas moisture content of 19%–22%.

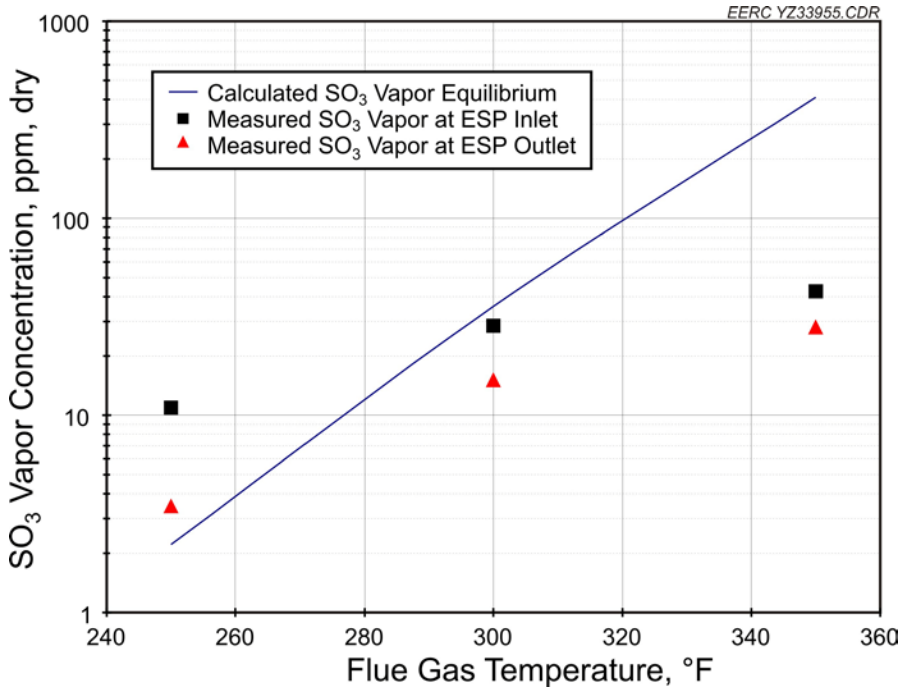

Figure 7. Comparison of measured SO_3 vapor concentration and the calculated equilibrium value as a function of flue gas temperature.

Mercury Speciation Across ESP at Different Moistures. The averaged CMM data corresponding to the different flue gas moisture testing conditions are presented in Table 8. No significantly improved native mercury removal was achieved with the increasing moisture in flue gas. The effect of moisture on mercury speciation is also not significant. Two separate trends are suggested with increasing moisture content, either the ESP inlet speciation remains constant while the outlet oxidized fraction increased or the inlet oxidized mercury decreased while the outlet oxidized mercury remained relatively stable. One consistent effect was that at high-moisture conditions, the decrease in oxidized mercury across the ESP observed in previous results appears to be cancelled out, and there was a smaller difference between the inlet and outlet speciation values.

Activated Carbon Injection at Different Moistures. ACI using DARCO Hg-LH was tested at high-moisture conditions, and the results are shown in Figure 8. The baseline (no moisture added) 8.5% data in Figure 8 are the same 300°F data presented in Figure 5. ACI performed slightly better in the higher-moisture conditions than the baseline case, e.g., with approximately 22% flue gas moisture, the mercury removal is greater than 40% at a ACI rate of 9.6 lb/Macf. However, the improved ACI performance with higher-moisture flue gas was not as good as that attained in flue gas at reduced temperature. Mercury speciation data at the ESP outlet during ACI testing are included in Table 8.

Table 8. Averaged CMM Concentration Data for the Moisture Testing

Flue Gas Moisture	ESP Inlet Total Hg, µg/dNm^3	ESP Inlet Elemental Hg, µg/dNm^3	ESP Inlet Percent Oxidized	ESP Outlet w/o ACI Total Hg, µg/dNm^3	ESP Outlet w/o ACI Elemental Hg, µg/dNm^3	ESP Outlet w/o ACI Percent Oxidized	ESP Outlet with ACI Total Hg, µg/dNm^3	ESP Outlet with ACI Elemental Hg, µg/dNm^3	ESP Outlet with ACI Percent Oxidized
8.5%	9.4	2.1	78	9.1	3.2	65	8.6[a]	3.5	60
19%	8.4	1.9	78	8.8	1.5	82	7.3[b]	1.7	77
22%	9.4	3.1	67	8.4	2.8	67	6.8[c]	2.2	67

[a] DARCO Hg-LH at a rate of 5 lb/Macf.
[b] DARCO Hg-LH at a rate of 6.8 lb/Macf.
[c] DARCO Hg-LH at a rate of 6.8 lb/Macf.

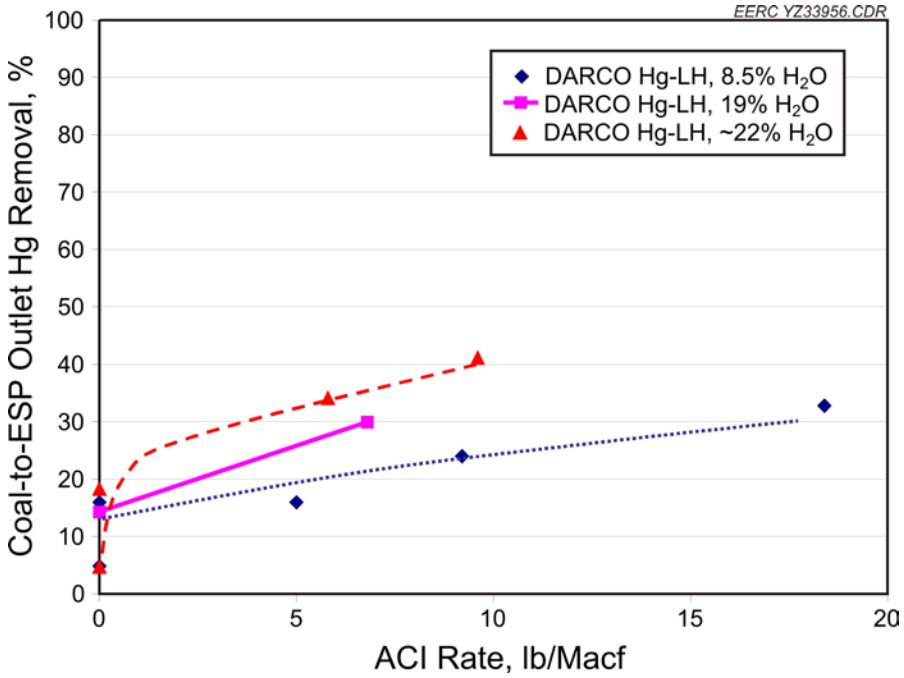

Figure 8. Summary of ACI testing with varying flue gas moisture levels.

SO_3 Partitioning. Flue gas SO_3 measurements were made at the elevated moisture conditions and are summarized in Figure 9. Because of the wide variability observed in these results, the ESP inlet measurements have not been averaged together as they were in Figure 6. In general, the total amount of SO_3/H_2SO_4 for the elevated moisture conditions is higher than the 131-ppmv average identified for the flue gas temperature test series, and the partitioning of SO_3 vapor to H_2SO_4 aerosol appears variable since the total amount of SO_3 and H_2SO_4 was not consistent under different moisture conditions. Possible reasons for these results could be that the steam injection at the combustor outlet altered the flue gas composition or the SO_3 sampling was affected by moisture addition.

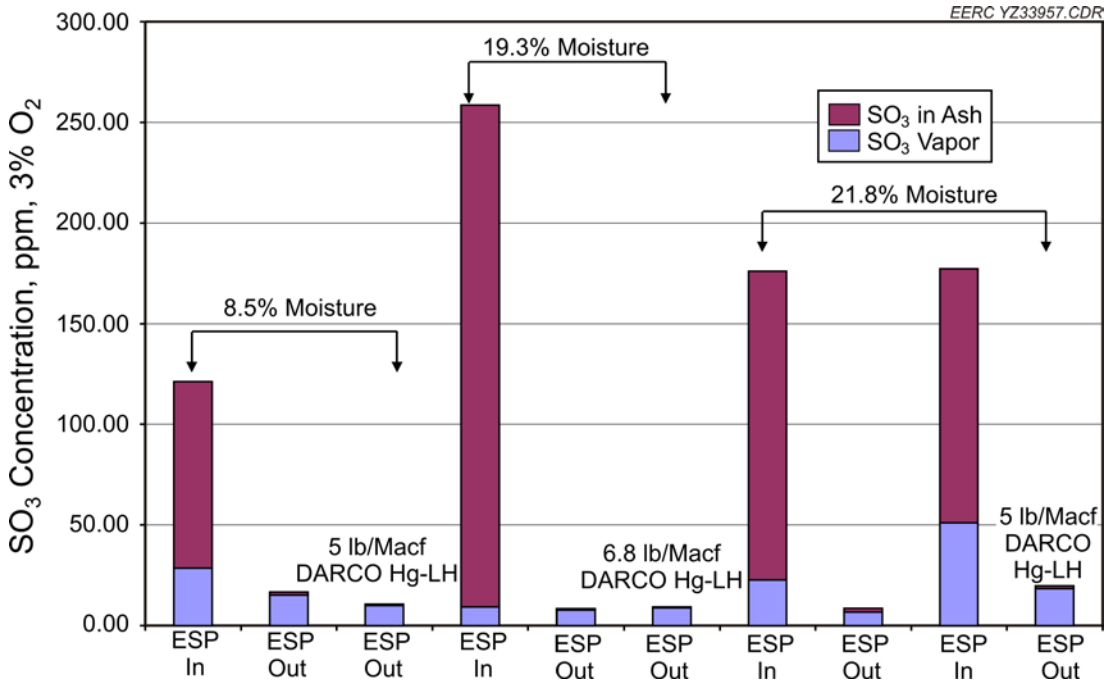

Figure 9. SO_3 concentration measurements for the flue gas moisture testing.

Removal of most of the aerosol form and a portion of the vapor form across the ESP does appear to be consistent with other SO_3 measurements.

A comparison of the measured SO_3 vapor concentrations has been made to calculated equilibrium values and is shown in Figure 10. As indicated in the figure, agreement with the equilibrium calculation was fair, but some measured data clearly do not agree well. It may be that moisture addition unpredictably affected either the actual SO_3 concentrations or the measurement technique.

Regardless of whether the measured SO_3 concentrations during moisture testing can be fully explained, the effect of flue gas moisture level on Hg capture with ACI seems minor compared to the effect of changing flue gas temperature. Equilibrium calculations indicate that there would be approximately a 25-ppmv change in SO_3 equilibrium concentration over the moisture content range of 8%–22%; compared to the 2–400-ppmv SO_3 change calculated for a 250°–350°F temperature variation; the effect of moisture on SO_3/H_2SO_4 partitioning is not as significant. This is qualitatively substantiated by the resulting effects on mercury control with moisture injection (Figure 8) compared to those of Figure 5 for flue gas temperature variation.

Alkali Injection. Injection of additives that have an alkali metal active ingredient was evaluated for the effect on mercury control and SO_3 distribution. Alkali materials have been injected into the air preheater inlet for SO_3 reduction but with the concern of ash fouling and plugging within the air preheater (9). In this pilot-scale study, the EERC has treated the alkali materials with its proprietary technology to enhance the reactivity of the

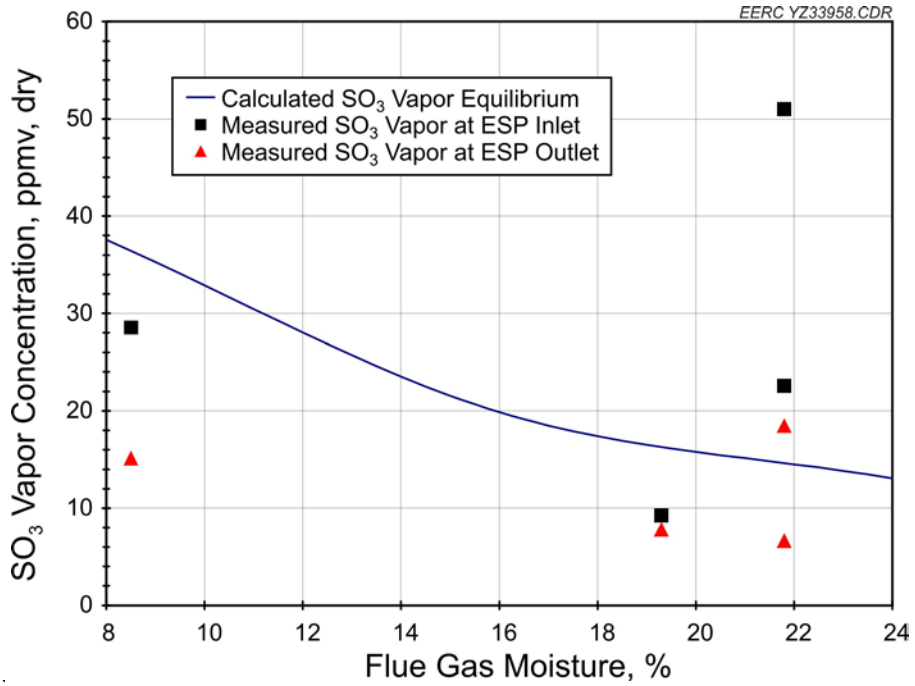

Figure 10. Comparison of measured SO_3 vapor concentration and the calculated equilibrium value as a function of flue gas moisture level.

alkali materials to be fully utilized for SO_3 reduction in flue gas, labeled as Alkali I. The details of the EERC proprietary approach can be found elsewhere and will not be discussed (10). It should be noted that the data presented here apply only to the EERC's method of alkali injection and do not imply a fundamental relationship between the alkali/SO_3 ratio that would hold true for all alkali materials or application methods. A dry Na_2CO_3 injection, labeled as Alkali II, was also tested for comparison.

Alkali injection was performed upstream of the ESP but downstream of the ESP inlet CMM and SO_3-sampling points, so mercury and SO_3 sampling at the ESP inlet was not affected by alkali injection.

Mercury Emissions with Alkali Injection. Since ESP inlet mercury sampling was not affected by alkali injection, the measured inlet mercury data were consistent with previous results at 300°F. ESP outlet total and elemental mercury concentrations with alkali injections are summarized in Table 9. Given the range of percent oxidation values observed with no alkali injection (i.e., molar ratio values of zero in Table 9), there appears to be no strong effect of alkali injection alone on the oxidation of mercury.

Mercury Emissions with a Combination of Alkali Injection and Activated Carbon Injection. ESP outlet total and elemental mercury concentrations with both Alkali Injection and ACI into the ESP are also included in Table 9. As suggested by the ESP outlet mercury values of Table 9, the injected Alkali I material significantly facilitated mercury removal with ACI. Compared to ESP outlet total mercury values of 8.5 μg/dNm^3 (average) and 7.5 μg/dNm^3 for baseline and Alkali I injection alone (Alkali I/SO_3 vapor=

6.8), respectively, a combination of 5-lb/Macf DARCO Hg-LH and Alkali I injection at 9.2 Alkali I/SO_3 vapor mole ratio reduced mercury emissions at the ESP outlet to 2.4 μg/dNm^3.

Table 9. Averaged ESP Outlet CMM Data for the Alkali Injection Testing

Alkali I/SO_3 Vapor Molar Ratio	Total Hg, μg/dNm^3	Elemental Hg, μg/dNm^3	Percent Oxidized
Alkali I injection Only, no ACI			
0.0	8.4	2.0	76
0.0	9.2	3.1	67
0.0	7.6	2.9	62
0.5	8.9	2.3	74
1.7	8.2	3.2	61
2.5	8.9	2.6	71
4.9	7.4	2.9	61
6.8	7.5	2.7	64
Alkali I Injection with 5 lb/Macf DARCO Hg-LH ACI			
0.0	8.7	2.8	68
1.7	5.4	1.4	74
1.7	6.1	2.7	55
9.2	2.4	1.5	60[a]
13.7	2.2	0.8	61

[a] The CMM-derived oxidation value was 38% and was not consistent with other results, therefore, the corresponding OH-derived oxidation value has been substituted.

A summary of the mercury removal data of alkali injection, with and without ACI, is presented in Figure 11. As shown in Figure 11, Alkali I injection alone moderately improved the native capture of mercury across the ESP; mercury removal was increased to a maximum value near 30%. The combination of Alkali I injection and ACI, on the other hand, showed a dramatic improvement and resulted in the highest mercury removal levels observed during the pilot-scale testing. With an Alkali I-to-SO_3 ratio near 2 and ACI at 5 lb/Macf, mercury removals were between 40% and 50%, which was roughly equivalent to the equivalent results from the 250°F testing. At higher Alkali I-to-SO_3 ratios, mercury removal reached a plateau of slightly less than 80%.

Figure 11 also includes mercury testing results with 5 lb/Macf ACI combined with Alkali II injection at a molar ratio of alkali/SO_3 of 13.7. A 44% mercury capture across the ESP was achieved under these conditions, which is higher than the 15%–20% mercury removal attained by 5 lb/Macf ACI alone under the same flue gas conditions (300°F with 8.5% moisture) but is much lower than the 80% mercury capture using a combination of Alkali I and ACI at the same injection rate. This result indicates the importance of the appropriate form and sufficient reactivity added species must have to effectively

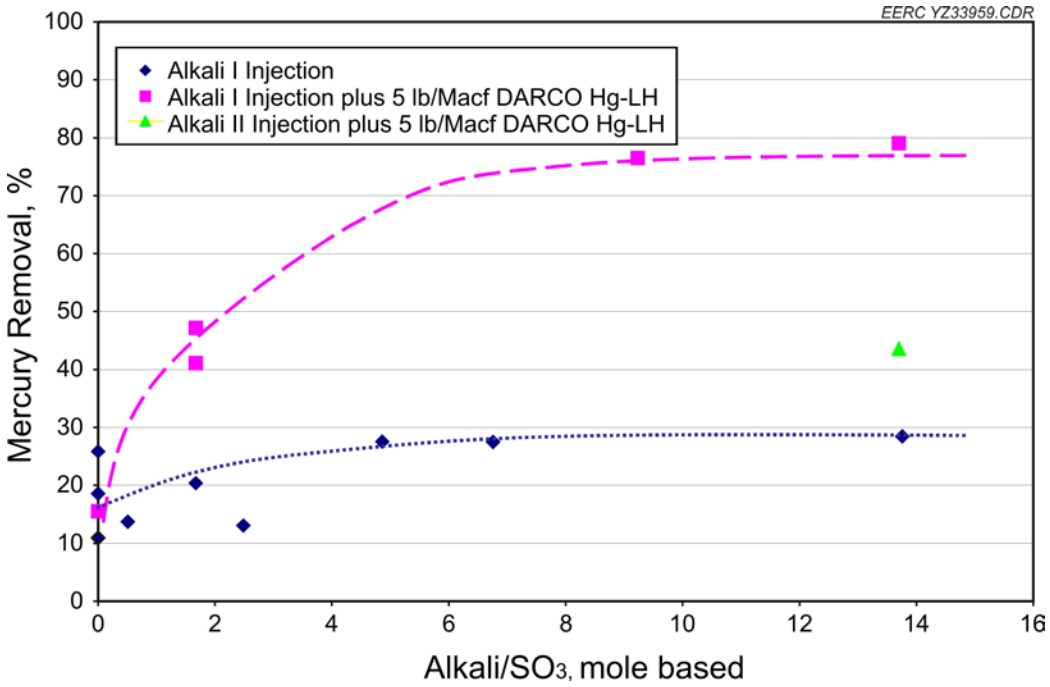

Figure 11. Summary of mercury removal data for the alkali injection testing.

neutralize SO_3 in the short contact time available and, subsequently, benefited mercury capture with ACI.

Partitioning SO_3 with Alkali Injection. The flue gas SO_3 measurements made during Alkali I injection testing are presented in Figure 12. The ESP inlet measurements were not affected by the alkali injection, and they are consistent with previous baseline SO_3 measurements. For instance, the total amount of SO_3/H_2SO_4 for the inlet samples is fairly steady and close to the 131-ppmv average obtained from the flue gas temperature test series (Figure 5). Furthermore, the partitioning between vapor and aerosol is steady and is also consistent with the 300°F sample from Figure 5. All ESP outlet SO_3 values were similar in that very little SO_3/H_2SO_4 was detected in any of the outlet samples, regardless of the alkali-to-SO_3 molar ratio or the addition of ACI. Previous data in Figures 6 and 9 indicate that the aerosol H_2SO_4 was already effectively removed across the ESP, and in the data of Figure 12, it was observed that the addition of even the lowest amount of alkali tested resulted in efficient removal of the SO_3 vapor as well.

The experimental data on alkali injection tests again prove the hypothesis that SO_3 vapor is the predominant factor that impedes efficient mercury removal with AC in an Illinois coal flue gas, while SO_3 aerosol (H_2SO_4 mist) has less impact on ACI performance.

Trace Element Sampling. The trace elements of interest, mercury, selenium, and arsenic, were sampled at three temperature regimes, 800°, 425°, and 312°F, to investigate their transformation following the combustor. EPA M29 sampling of the flue gas was performed to measure the total amount and partitioning of each element in the flue gas. These results are provided in Table 10 for the elements of interest.

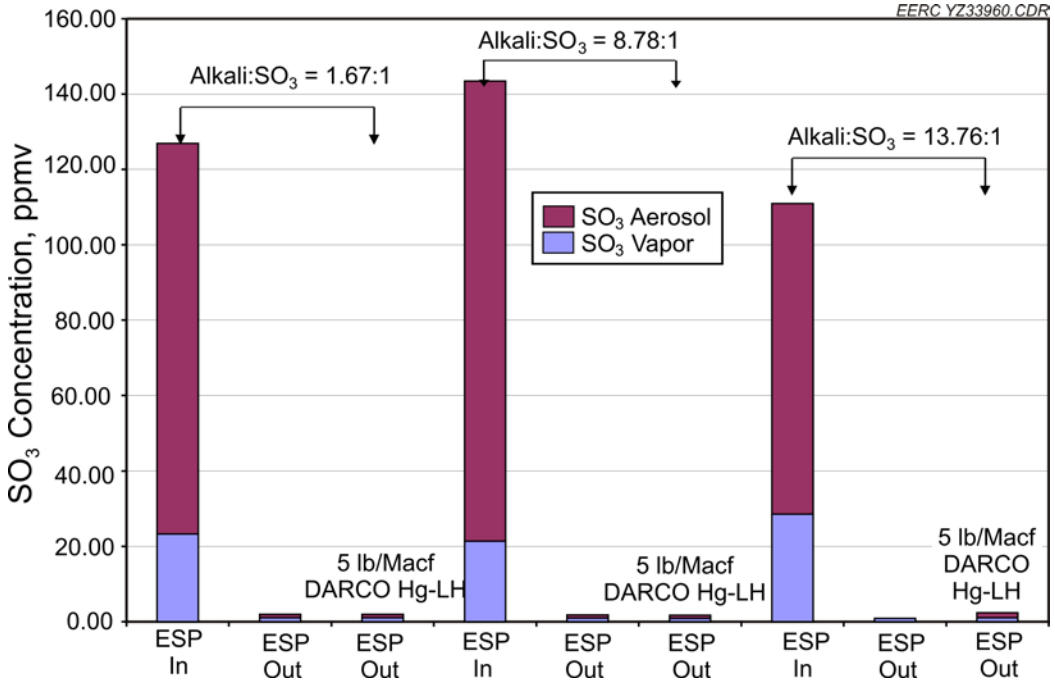

Figure 12. SO_3 sampling results for the Alkali I injection testing.

Table 10. Distribution of Mercury, Selenium, and Arsenic in the Flue Gas at Temperatures of 800°, 425°, and 312°F

Flue Gas Temperature, °F	Gas Phase, μg/dNm^3	Particulate, μg/dNm^3	Total, μg/dNm^3	Percent in Gas Phase
Mercury				
800°	8.22	0.0128	8.24	99.8
425°	9.34	0.0231	9.37	99.8
312°	10.2	0.0148	10.2	99.9
Selenium				
800°	90.2	17.3	107	83.9
425°	77.7	120	198	39.3
312°	61.4	96.4	158	38.9
Arsenic				
800°	4.46	334	338	1.3
425°	1.41	368	369	0.4
312°	1.61	339	341	0.5

As the results in Table 10 show, mercury was found almost exclusively in the vapor phase for all temperatures, and the total amounts of mercury are consistent with other baseline ESP inlet data. For selenium, however, this temperature profile does capture the transformation of vapor-phase material to particulates, somewhere between 800° and 425°F. Arsenic was at the other extreme; by the time the flue gas cooled to 800°F, it had largely already become particulate-bound, although the measurements do suggest that this process does not completely end until somewhere between 800° and 425°F.

Mass balance calculations were performed to determine what fraction of the trace elements entering the system in the coal were quantified by the M29 measurements. These results are presented in Table 11. The mass balance values are presented as the ratio of the total concentration measured in the flue gas to the amount of the element entering in the coal. Some variability is expected with mass balance calculations, and closure within ±20% is considered good. As indicated in Table 11, mercury and arsenic have closure values near 100%, implying that all of the mercury and arsenic entering the system with the coal was detected in the flue gas at the various sampling points. This is not unexpected since these elements are relatively volatile and would not normally remain within bottom ash.

However, the closure values for selenium are much lower; this might indicate that some of the selenium was not released to the gas phase in the combustor, but considering that selenium is volatile at combustion temperatures, it is probable that the flue gas measurements are biased low. Selenium is considered a semivolatile trace element, meaning that selenium species remain in the vapor phase at high temperature, e.g., 800°F, but become particulate-bound with decreasing temperature as shown in Table 10. The transition from vapor to particulate may result in partial selenium vapor condensation along sampling lines which might not be fully recovered during analysis and would, therefore, cause an underestimation of the vapor-phase selenium.

Table 11. Mass Balance Values for the Trace Element Sampling

Flue Gas Temperature, °F	Mass Balance Closure[a], %
Mercury	
800°	82
425°	93
312°	102
Selenium	
800°	32
425°	58
312°	47
Arsenic	
800°	97
425°	106
312°	98

[a] Calculated as the ratio of the mass flow rate of the element in the flue gas to the flow rate entering with the coal. Assumed flue gas flow of 119 dscfm and an as-received coal feed of 55 lb/hr.

To gain insight into the particulate-forming mechanisms, the fly ash particle-size distribution was also measured at each flue gas temperature. The size distributions are plotted together in Figure 13. Each measurement indicates a bimodal size distribution, with one peak in the particle size range of 0.2–0.5 μm and the other at approximately 10 μm. The most significant change among the measurements is between the temperatures of 800° and 425°F, where the bimodal peaks become more clearly defined and separated. It would appear that some of the submicrometer particulates at 800°F were continuing to agglomerate and form larger particles. The more consistent size

distributions from 425° to 312°F suggest that the particulate formation phase was mostly complete by 425°F.

The particulate samples collected during the size distribution measurements of Figure 13 were analyzed for the trace elements that were found as particulates in significant amounts, i.e., selenium and arsenic. This adds the dimension of trace element concentration as a function of particulate size to the trace element analysis. The results are plotted in Figures 14 and 15 for selenium and arsenic, respectively. It should be noted that mercury concentrations of the size-segregated fly ash samples were below instrument detection limit, which is consistent with EPA M29 results.

Both elements in Figures 14 and 15 show some enrichment in submicrometer-sized particles. For selenium, the 800°F concentration data are noticeably less than at the lower temperatures, which agrees well with the fact that primarily vapor-phase selenium was detected in the flue gas at that condition. The data suggest that as the selenium cooled and became particulate-bound, it preferentially formed or became attached to very fine particles. This may support a condensing aerosol model, but is also indicative of the relative rates of mass transfer between small and large particles and the resulting overall particle selenium concentration.

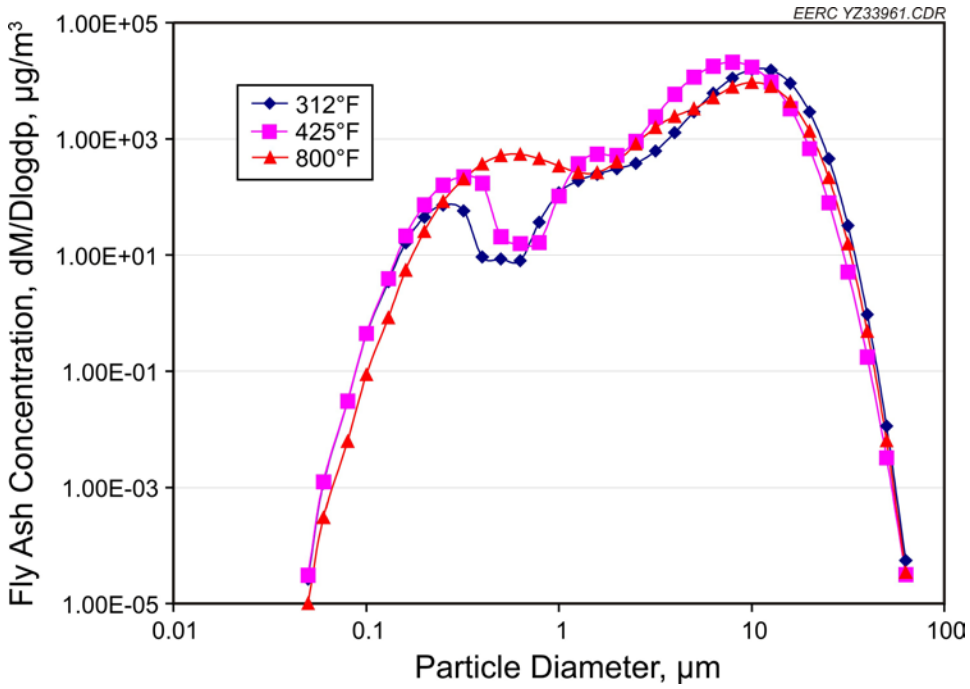

Figure 13. Fly ash size distributions for the three flue gas temperatures investigated.

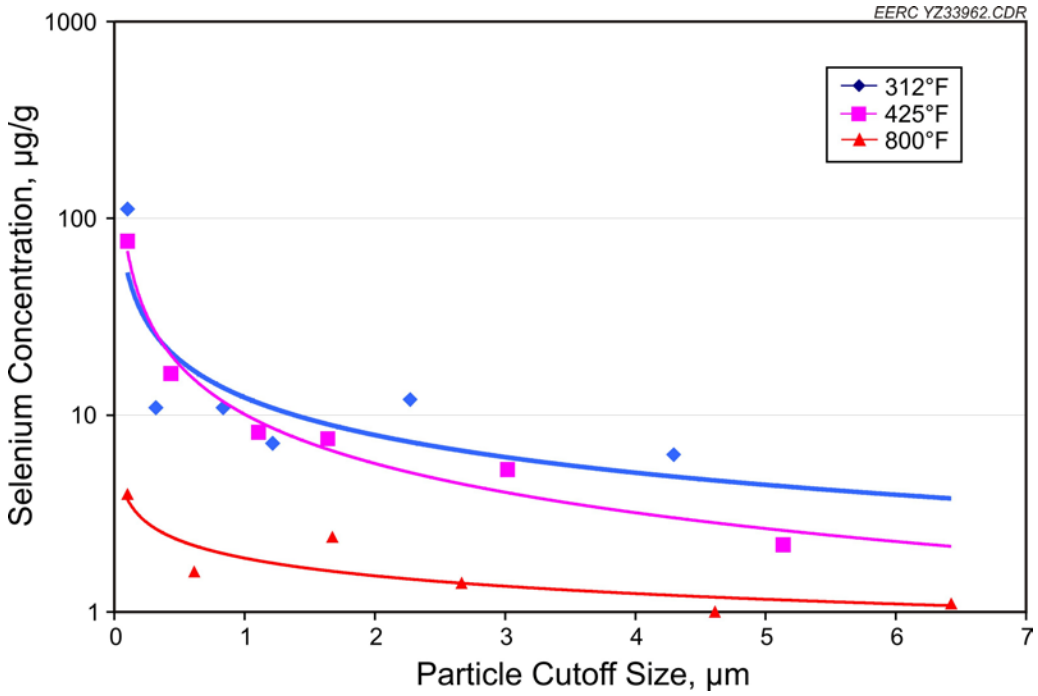

Figure 14. Selenium concentration as a function particulate size.

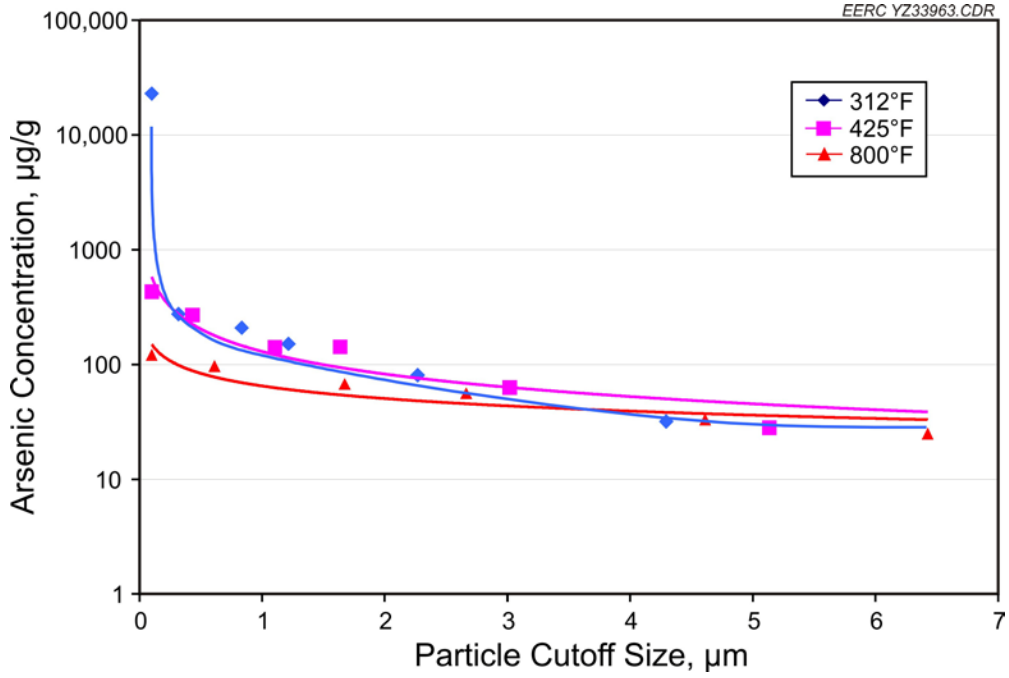

Figure 15. Arsenic concentration as a function particulate size.

The data for arsenic in Figure 15 show a much more subtle transition from gas phase to particulate-bound and are, again, supportive of the flue gas measurements which indicated that most of the arsenic had become particulate-bound prior to 800°F. The data indicate that for particles above 2 μm, arsenic concentrations are quite uniform for the temperatures from 312° to 800°F, while the enrichment in the submicrometer particles continues to occur all the way to 312°F. The relative concentration difference between the submicrometer particles and those greater than approximately 2 μm was roughly two orders of magnitude, c.a. 10,000 μg/g versus 100 μg/g for arsenic, while the same ratio was only approximately one order of magnitude for selenium.

Discussion

Mercury Control. Pilot-scale testing data indicate that while some variability was observed during the tests, native mercury removal was estimated to be less than 10% across the ESP under the baseline Illinois coal flue gas conditions (300°F with 8.5% moisture). Mercury speciation in the baseline flue gas was approximately 79% and 64% oxidized at the ESP inlet and outlet, respectively. It was observed that the coal chlorine content was lower than expected for an Illinois coal, and it is possible that the lower chlorine content limited mercury oxidation. This phenomena is characteristic of coals with much lower chlorine contents, e.g., lignite and subbituminous, which typically emit a high fraction of elemental mercury. Mercury oxidation with these coals has been enhanced with additional coal chlorine content, but Illinois coals typically have very high chlorine, and this should not normally be a concern. A significant factor regarding the mercury oxidation results is that the configuration for the pilot-scale work did not include a SCR unit, which can substantially enhance mercury oxidation. For those plants without a SCR unit or otherwise needing enhanced mercury oxidation, injection of suitable oxidants has been shown to be effective and would likely be another choice. Although not tested here, these oxidants could increase mercury oxidation and result in improved cobenefit mercury removal in a wet FGD.

Mercury removal was also evaluated using AC sorbent injection. Baseline pilot-scale testing showed that ACI did not perform well in Illinois coal flue gas; only a 33% mercury capture was attained with the ESP at an extremely high injection rate of 18.4lb/Macf DARCO Hg. The hypothesis proposed in this work is that the SO_3 vapor generated from combustion of high-sulfur coal reacted with the carbon and hindered its ability to remove mercury. This necessitated a thorough understanding of multi-interactions among mercury, SO_3, and carbon under different flue gas conditions: temperature, moisture content, and particulate alkali content.

Pilot-scale testing data indicate that, by individually changing flue gas temperature, moisture level, and alkali content alone, mercury oxidation and removal across the ESP were not significantly improved. A maximum 10%–25% mercury removal by the ESP was achieved when Alkali I was injected into the flue gas as shown in Figure 11.

However, lowering flue gas temperature, increasing moisture level, and Alkali I material injection dramatically enhanced ACI in-flight mercury capture performance in the pilot-

scale configuration. Measurements of SO_3 vapor/H_2SO_4 aerosol as a function of parametric test conditions did show consistency with the expected trends. When the complete set of data are examined, including the mercury capture trends with ACI, the parametric data appear to support the hypothesis that it is SO_3 vapor which hinders mercury capture with AC, while H_2SO_4 aerosol has much less impact on in-flight mercury capture of ACI.

As an example, the effect of flue gas temperature on SO_3 vapor concentrations can be considered (Figure 6). While the total amount of SO_3 vapor and H_2SO_4 aerosol remained relatively consistent for all of the inlet samples, the ratio of SO_3 to H_2SO_4 varied as a function of temperature, i.e., more SO_3 vapor with increasing temperature. When examining the corresponding ACI testing (Figure 5), there was a clear negative effect with increasing temperature, especially between 250° and 300°F, suggesting that mercury capture with ACI was clearly more sensitive to the SO_3 vapor fraction than to the amount of H_2SO_4 aerosol. Another conclusion might be that mercury capture with AC was, instead, sensitive to flue gas temperature, but this conclusion is not consistent with mercury removal results with different coals, especially those with lower sulfur content and inherently lower amounts of SO_3. A similar relationship can be observed with the flue gas moisture test series data of Figure 8, which shows better mercury removals with higher moisture. The improvements are not as significant as those from the temperature test series, but the equilibrium calculations predict a correspondingly smaller reduction in SO_3 vapor from increasing moisture (Figure 10), compared to decreasing temperature (Figure 7).

By assuming that SO_3 vapor is the key factor limiting carbon performance, it was possible to resolve data from all of the parametric testing on the basis of SO_3 vapor concentration alone. This relationship is presented graphically in Figure 16, which is a plot of mercury removal with ACI versus the corresponding SO_3 vapor concentration at the same flue gas conditions but with no ACI. The corresponding, no-ACI SO_3 concentrations were used in Figure 16 because they were the most representative measurements of SO_3 concentration at the point of carbon injection.

The trend in Figure 16 is remarkably consistent considering that the SO_3 concentration was manipulated using three completely different techniques: flue gas temperature variation, moisture addition, and injected alkali material. Figure 16 suggests an exponential decline in AC performance with increasing SO_3 vapor concentration. Above approximately 10 ppmv, the deleterious effect on carbon performance has saturated and the mercury removals settle at 18%–19% for an ACI rate of 5 lb/Macf. For SO_3 vapor concentrations below 10 ppmv, the improvement in carbon performance is dramatic with decreasing SO_3 concentration.

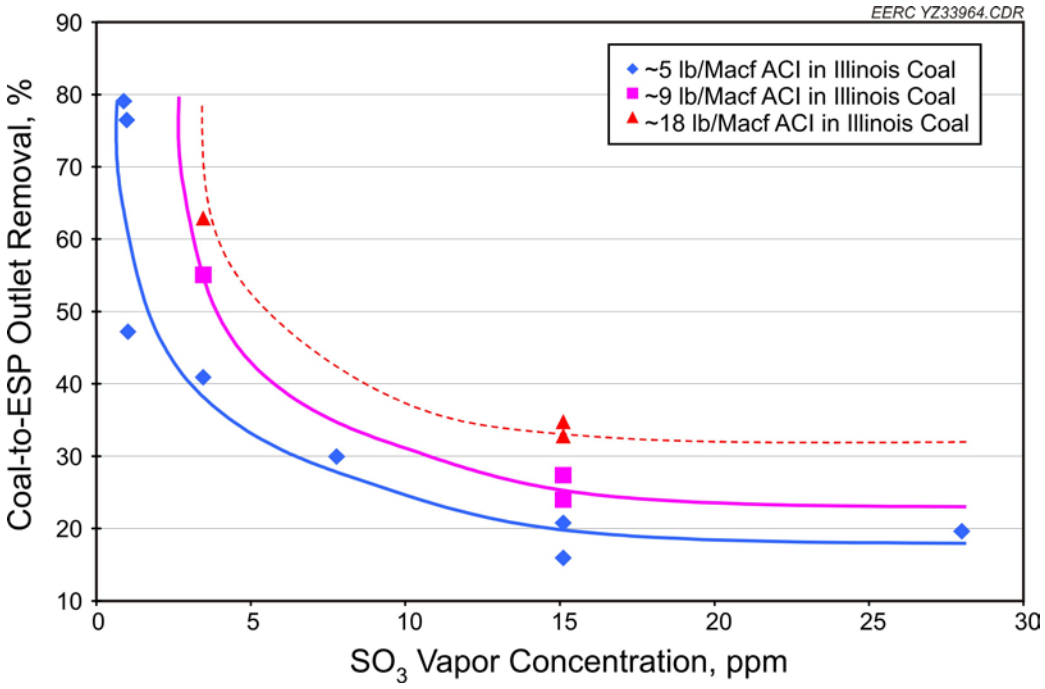

Figure 16. Relationship between mercury removal with ACI and the corresponding SO_3 vapor concentration.

Mass transfer modeling of the SO_3 adsorption process was performed to qualitatively investigate the results of Figure 16. Transportation of bulk gas species to in-flight sorbent can be described using Equation 1:

$$\frac{dC_i}{dt} = -k_g \frac{a}{V}\left(C_i - C_i^*\right) \qquad \text{[Eq. 1]}$$

where C_i is the gas-phase concentration of species *i*; k_g is the mass transfer coefficient of gas-phase species *i* to the in-flight sorbent; *a/V* is the total surface area of sorbent per unit volume of flue gas; and C^*_i is the equilibrium vapor concentration of the adsorbed species *i* and was set to zero by assuming the injected sorbent acted as a sink for SO_3 vapor and mercury. The mass transfer coefficient for the gas-phase diffusion of a species *i* to the surface of a sorbent particle can be estimated using Equation 2:

$$k_g = \frac{2 \cdot D_i}{d_p} \qquad \text{[Eq. 2]}$$

where D_i is the diffusivity of species *i* in flue gas and d_p is the diameter of sorbent particle. Given that the diffusivities for mercury and SO_3 are 0.251 cm^2/s and 0.221 cm^2/s at 300°F, respectively, their overall mass transfer coefficients are roughly equivalent for transport to a specific particle size. According to Equation 1, this implies that the rates of mass transfer of mercury and SO_3 to the same particles of AC would then be directly proportional to the concentration of these species in the flue gas, i.e., C_i.

The relationship between the relative concentration of mercury to SO_3 vapor has been plotted in Figure 17 for the conditions of the pilot-scale testing. As shown in the figure, the mercury relative to SO_3 decays exponentially with increasing SO_3 level. Assuming there are a finite number of sites on the carbon suitable to capture either mercury or SO_3, the trend of Figure 17 suggests that as SO_3 levels rise, the quantity of mercury occupying those sites would decrease sharply; this is exactly the trend shown by the experimental data in Figure 16.

Further calculations were performed to determine if the mass transfer trends suggested in Figure 17 could characterize the experimental data. A model was created that used input values based on the pilot-scale testing, e.g., carbon injection rate, residence time, carbon particle-size distribution, and carbon particle density. The model used a finite difference form of Equation 1, shown as Equation 3, to calculate the mercury and SO_3 capture for each particle size during each time step, Δt.

$$\Delta C_i = -k_g \frac{a}{V}(C_i)\Delta t \qquad \text{[Eq. 3]}$$

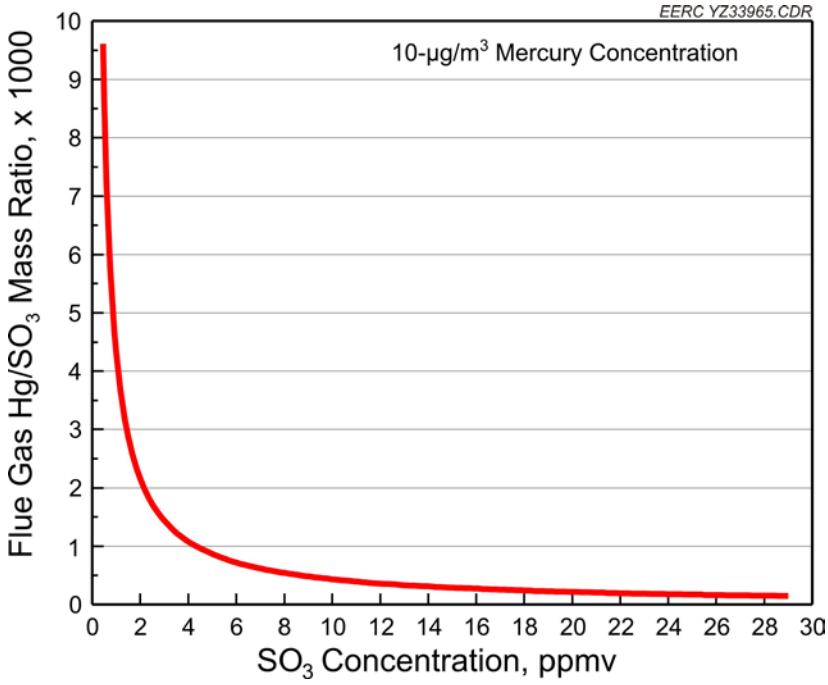

Figure 17. Mass ratio of mercury to SO_3 for relevant flue gas conditions.

As shown in Equation 3, it was assumed that the equilibrium vapor concentration of adsorbed mercury and SO_3 was zero, indicating no counterdiffusion or release of mercury or SO_3 from the particle's surface to the flue gas. Furthermore, no surface reaction kinetics were included, and the reaction times required for mercury and SO_3 capture were assumed to be equal and instantaneous relative to the simulation time increment. These

assumptions limit the application of the model to cases where mercury capture is mass transfer-limited, typically at low ACI rates.

In order to represent the finite number of sites on the AC available for mercury and SO_3 capture, the model included a limit on the total adsorption of mercury and SO_3 per unit of carbon surface area. This parameter was not an intrinsic property of the carbon, but is instead the mercury and SO_3 capacity of the carbon available under the mass transfer conditions of the test, i.e., it is a function of sorbent loading, mercury concentration, and residence time in addition to the active sites available on the carbon. This parameter was determined empirically from the pilot-scale results.

Results from the mass transfer modeling are compared with the experimental data in Figure 18. As shown in the figure, the mass transfer model accurately represents the observed data for a 5-lb/Macf ACI rate for all except the highest SO_3 concentration. The maximum possible removal based on mass transfer limitations was calculated to be approximately 80% and is in good agreement with the highest removal values observed during testing. As SO_3 concentration increases, the mass transfer modeling results in a sharp decay of mercury removal which continues to fall until it is less than 10% at an SO_3 concentration of 30 ppmv. This is approximately 10 percentage points lower than the experimental data point at 28 ppmv SO_3 and may be explained by the fact that no native removal was considered in the model.

The mass transfer modeling of mercury and SO_3 transport to the AC provide confirming evidence that there is a direct competition between mercury and SO_3 for the active sites on the carbon. The mass transfer calculations show that an SO_3 concentration of approximately 4 ppmv would reduce mercury capture by 50% compared to the same conditions but with no SO_3. Considering that AC is the most significant contribution to the levelized cost of mercury removal with ACI (11), injecting additional carbon to compensate for SO_3 poisoning will not be a cost-effective solution. Among the flue gas parameters explored, lowering the flue gas temperature may cause enough SO_3 vapor to form an aerosol so that the AC can work effectively. In practical application though, the operating exhaust temperatures of a plant's flue gas have been carefully selected based on several plantwide factors, including plant efficiency, emissions, and corrosion concerns. While the advent of mercury control may change this analysis somewhat, lowering temperatures would also cause a host of unintended and possibly unwanted consequences.

Injection of a suitable material to react with and negate the SO_3 vapor appeared to be the most feasible and best-performing option provided that the material is sufficiently reactive and has the mobility to fully interact with the SO_3. The results indicate that alkali injection at the lowest rate tested, i.e., an alkali-to-SO_3 molar ratio of 1.67, resulted in near complete removal of SO_3 vapor following the ESP (see Figure 12). However, this leaves the curious result of why mercury capture continued to improve with additional alkali injection if all of the SO_3 vapor was apparently removed with the lowest injection rate. It would seem that even with alkali injection, the AC was still capturing some of the

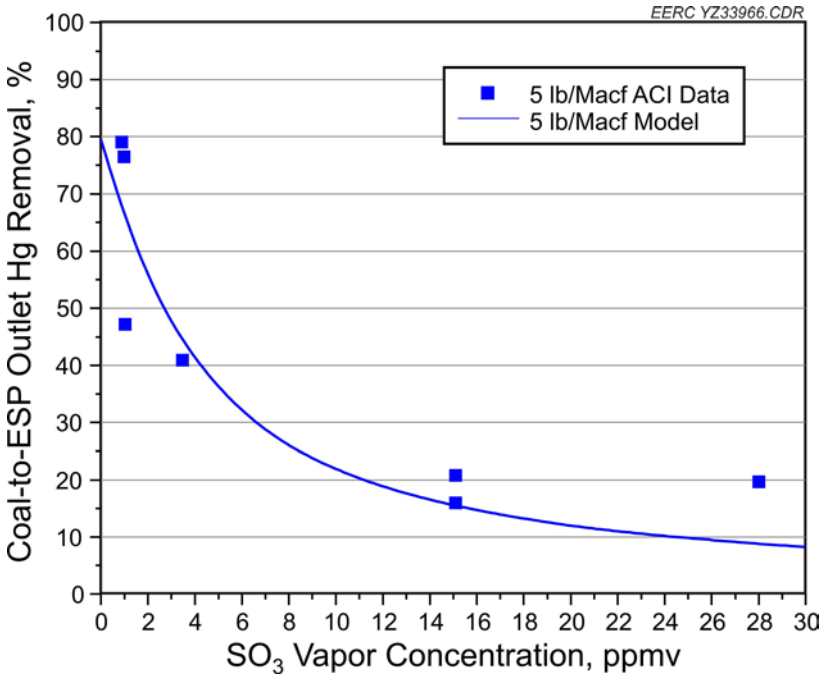

Figure 18. Comparison of measured removal data and mass transfer model results.

SO_3 vapor at the lower alkali injection rates, i.e., the alkali and AC were essentially "competing" for SO_3 vapor. By increasing the rate of alkali injection, the rates of mass transfer were shifted so that more SO_3 was intercepted by the alkali, leaving the AC more surface area and time to capture mercury. This emphasizes the point that SO_3-neutralizing material must not only be reactive toward SO_3 vapor, but must also have a higher rate of SO_3 mass transfer than the AC to be effective.

Enhancing mercury oxidation does not appear that it will improve native removal since the mercury was already entering the ESP with a high oxidized fraction. Therefore, unless a plant has significant unburned carbon in the flue gas, which was purposely minimized during the pilot-scale testing, enhancing native removal does not appear to be a viable control option.

Trace Element Distribution. The partitioning of trace elements between vapor and particulate phases and their relative distribution within the particulates were measured to determine the transformation that these elements undergo following the combustor to the particulate control device. The trace elements were selected based on the interests of Illinois coal users and represent the most volatile trace contaminants of coal: mercury, selenium, and arsenic.

The trace element partitioning data show that mercury remains as a vapor and is not significantly condensed at the temperatures relevant to a power plant's flue gas exhaust. This is the underlying reason why vapor-phase mercury control strategies have been developed, e.g., chemisorption with AC or conversion into a water-soluble form (oxidation) for capture in a wet FGD unit.

Some conversion of selenium to the particulate phase occurred at temperatures between 800° and 425°F; however, the transition was not complete and approximately 61 μg/Nm^3 of selenium vapor was detected at the ESP inlet temperature (312°F), accounting for ~40% of total selenium in coal flue gas. Selenium emissions past the ESP were not directly measured for this work, but based on previous experience at full-scale plants (12), selenium vapor is not captured effectively by particulate control devices or in wet FGD systems, and some portion of the detected selenium vapor would be expected to be emitted. In the referenced work (12) approximately 60% of the selenium in the coal was captured in a plant utilizing a cold-side ESP and wet FGD system.

If it becomes necessary to regulate selenium, it appears that some vapor-phase control technology will need to be developed, as it has for mercury, to achieve removals above 50%–70%. AC has been shown to have some affinity for selenium (13), but it does not appear to be as effective as it is for mercury control. Mass transfer rates limit the capture of selenium vapor in wet FGD systems, although the cooler temperatures may cause some additional selenium to condense. Monitoring of selenium may also pose new challenges. The mass balance calculations presented in Table 10 had the lowest closure for selenium, highlighting possible issues with selenium vapor sampling. While detailed measurement and control of selenium is in its relative infancy compared to the advances made for mercury emissions, these data suggest that control (beyond any cobenefit removal) and measurement of selenium will not be trivial tasks.

Arsenic's conversion to a particulate primarily occurred above 800°F, and while emissions were not directly measured, past experience indicates that the particulate-bound arsenic will be removed effectively by an ESP or other particulate control device. However, judging from the arsenic concentration data of Figure 15 and the mass-based particle-size distribution of Figure 13, it seems that the submicrometer particulates are highly concentrated with arsenic. Therefore, for effective arsenic abatement, the particulate control device should collect these small particles with high efficiency.

CONCLUSIONS AND RECOMMENDATIONS

A pilot-scale combustion test was conducted with a representative Illinois Basin coal; the cold-side ESP-only configuration was evaluated for mercury speciation and capture, SO_3 distribution, and transformation of trace elements of interest: mercury, selenium, and arsenic. The key findings relative to plants that fire Illinois coal can be summarized as follows:

- Native removal of mercury across the ESP was observed to be less than 10%, and it was not sensitive to any of the parametric test conditions, i.e., temperature, moisture level, or alkali injection. Unless a plant using Illinois coal has a significant amount of unburned carbon in the flue gas, native mercury removal will not be a significant contribution to overall mercury control.

- Mercury exiting the ESP was approximately 65% oxidized. Even with ACI, no increases to mercury oxidation were observed. The highest 78% mercury oxidation was observed during the 350°F testing. Significantly more oxidation could be expected for systems employing an SCR unit (which was not included in the pilot-scale configuration).

- The experimental data support the concept that SO_3 vapor is the predominant factor that impedes efficient mercury removal with AC in an Illinois coal flue gas, while H_2SO_4 aerosol has less impact on ACI performance. Mass transfer modeling of in-flight mercury capture suggests that there is a direct competition between mercury and SO_3 for active sites on the carbon.

- Although reducing flue gas temperature or increasing moisture level can counteract the deleterious effect of SO_3 vapor on ACI performance to some degree, injection of an additional material to neutralize the SO_3 vapor seems most promising. However, it is critical that the added material has sufficient reactivity and mobility to neutralize SO_3 in the short contact time available.

- The selenium transformation measurements indicate that while some of the selenium becomes particulate-bound, there was still around 40% selenium that remains as vapor at the ESP inlet temperature of 312°F. If selenium emissions become regulated, this fraction of selenium vapor may be very difficult to capture and would likely require the development of new technology.

- Transformation measurements for arsenic indicate that over 98% of the arsenic becomes particulate-bound by a temperature of 800°F and further reaches 99.5% at a temperature of 312°F. The arsenic was highly concentrated in submicrometer particles, but it should be effectively controlled with existing particulate control equipment.

REFERENCES

1. Miller, C.; Feeley, T.; Aljoe, W.; Lani, B.; Schroeder, K.; Kairies, C.; McNemar, A.; Jones, A.; Murphy, J. Mercury Capture and Fate Using Wet FGD at Coal-Fired Power Plants. *DOE/NETL Mercury and Wet FGD R&D*, Aug 2006.

2. Sjostrom, S.; Campbell, T. Influence of SO_3 on Mercury Removal with Activated Carbon: Full-Scale Results. 10th Annual EUEC Conference, Tucson, AZ, Jan 24, 2007.

3. Cao, Y.; Duan, Y.; Kellie, S.; Li, L.; Xu, W.; Riley, J.T.; Pan, W.P. Impact of Coal Chlorine on Mercury Speciation and Emission from a 100-MW Utility Boiler with Cold-Side Electrostatic Precipitators and Low-NO_x Burners. *Energy Fuels* **2005**, *19*, 842–854.

4. Olson, Edwin S.; Crocker, Charlene R.; Benson, Steven A.; Pavlish, John H.; Holmes, Michael J. Surface Compositions of Carbon Sorbents Exposed to Simulated Low-Rank Coal Flue Gases. *Air Waste Manage. Assoc.* **2005**, *55* (6), 747–754.

5. Yan, R.; Gauthier, D.; Flamant, G. Partitioning of Trace Elements in the Flue Gas from Coal Combustion. *Combust. Flame* **2001**, *125*, 942–954.

6. Ito, S.; Yokoyama, T.; Asakura, K. Emissions of Mercury and Other Trace Elements from Coal-Fired Power Plants in Japan. *Sci. Total Environ*. **2006**, 397–402.

7. Oda, R.L.; DeVito, M.S. Controlled Condensation Method for Flue Gas SO_3 Measurements. Presented at the Formation, Distribution, Impact, and Fate of Sulfur Trioxide in Utility Flue Gas Streams Conference.

8. Banchero, J.T.; Verhoff, F.H. Evaluation and Interpretation of the Vapour Pressure Data for Sulphuric Acid Aqueous Solutions with Application to Flue Gas Dewpoints. *Inst. Fuel* **1975**, *June*, 76–80.

9. Fenger, M.L.; Winschel, R.A. *Multipollutant Emissions Control: Pilot-Plant Study of Technologies for Reducing Hg, SO_3, NO_x, and CO_2 Emissions*; Report for U.S. DOE Cooperative Agreement DE-FC26-01NT41181; CONSOL Energy, Inc., 2006.

10. Holmes, M.J.; Pavlish, J.H.; Zhuang, Y.; Benson, S.A.; Olson, E.S.; Laumb, J.D. Multifunctional Abatement of Air Pollutants in Flue Gas. U.S. Patent App. Serial No. 12/177,771, July 22, 2008, CIP of 11/220,810, Sept 7, 2005.

11. Jones, A.P.; Hoffmann, J.W.; Smith, D.N.; Feeley, T.J.; Murphy, J.T. DOE/NETL's Phase II Mercury Control Technology Field Testing Program, Preliminary Economic Analysis of Activated Carbon Injection, 2006.

12. *Determination of Trace Element Concentrations at an Eastern Bituminous Coal Plant Employing an SCR and Wet FGD*; Report for EPRI, Palo Alto, CA, U.S. Department of Energy, Pittsburgh, PA, and Center for Air Toxic Metals, Grand Forks, ND; 1015612, 2008.

13. Pavlish, J.H.; Laumb, J.D.; Jensen, R.R.; Thompson, J.S.; Martin, C.L.; Musich, M.A.; Pavlish, B.M.; Miller, S.J.; Hamre, L.L. *Baghouse Slipstream Testing* at *TXU's Big Brown Station*; Final Report for DOE NETL Agreement No. DE-FC26-98FT40321; April 2007.

DISCLAIMER STATEMENT

This report was prepared by Ye Zhuang, Energy & Environmental Research Center with support, in part, from grants made possible by the Illinois Department of Commerce and Economic Opportunity through the Office of Coal Development and the Illinois Clean Coal Institute. Neither Ye Zhuang and the Energy & Environmental Research Center nor any of its subcontractors, nor the Illinois Department of Commerce and Economic Opportunity, Office of Coal Development, the Illinois Clean Coal Institute, nor any person acting on behalf of either:

(A) Makes any warranty of representation, express or implied, with respect to the accuracy, completeness, or usefulness of the information contained in this report, or that the use of any information, apparatus, method, or process disclosed in this report may not infringe privately-owned rights; or

(B) Assumes any liabilities with respect to the use of, or for damages resulting from the use of, any information, apparatus, method or process disclosed in this report.

Reference herein to any specific commercial product, process, or service by trade name, trademark, manufacturer, or otherwise, does not necessarily constitute or imply its endorsement, recommendation, or favoring; nor do the views and opinions of authors expressed herein necessarily state or reflect those of the Illinois Department of Commerce and Economic Opportunity, Office of Coal Development, or the Illinois Clean Coal Institute.

Notice to Journalists and Publishers: If you borrow information from any part of this report, you must include a statement about the state of Illinois' support of the project.